Emerging Biosensing Technologies for the Diagnostics of Viral Infectious Diseases

Gözde Kabay, Jonalyn DeCastro, Alara Altay, Kasey Smith, Hsiang-Wei Lu,
Antonia McDonnell Capossela, Maryam Moarefian, Kiana Aran,* and Can Dincer*

Several viral infectious diseases appear limitless since the beginning of the 21st century, expanding into pandemic lengths. Thus, there are extensive efforts to provide more efficient means of diagnosis, a better understanding of acquired immunity, and improved monitoring of inflammatory biomarkers, as these are all crucial for controlling the spread of infection while aiding in vaccine development and improving patient outcomes. In this regard, various biosensors have been developed recently to streamline pathogen and immune response detection by addressing the limitations of traditional methods, including isothermal amplification-based systems and lateral flow assays. This review explores state-of-the-art biosensors for detecting viral pathogens, serological assays, and inflammatory biomarkers from the material perspective, by discussing their advantages, limitations, and further potential regarding their analytical performance, clinical utility, and point-of-care adaptability. Additionally, next-generation biosensing technologies that offer better sensitivity and selectivity, and easy handling for end-users are highlighted. An emerging example of these next-generation biosensors are those powered by novel synthetic biology tools, such as clustered regularly interspaced short palindromic repeats (CRISPR) with CRISPR-associated proteins (Cas), in combination with integrated point-of-care devices. Lastly, the current challenges are discussed and a roadmap for furthering these advanced biosensing technologies to manage future pandemics is provided.

1. Introduction

Within this millennium, several infectious diseases originated by viruses, including the highly pathogenic Asian avian (H5N1) Influenza A,[1] Zika,[2,3] Ebola,[4] Hepatitis B and Hepatitis C,[5] and coronaviruses.[3,6] Despite these viruses emerging in different geographic areas, they have become an undeniable threat to worldwide public health and economic burden. The coronaviruses (CoVs) include severe acute respiratory syndrome (SARS-CoV), Middle East respiratory syndrome (MERS-CoV), and especially the most recent SARS-CoV variant, SARS-CoV-2, which has caused the virulent, airborne, and infectious coronavirus disease 2019 (COVID-19) that continues to affect millions of people, resulting in the ongoing pandemic outbreak.[3,6–10] Considering that most of the described viral-based community spread infections occur through aerosols and fomites[11] transmitted by presymptomatic and asymptomatic people,[12] diagnostic methods for the early detection with high accuracy and on-site capability are crucial and would further aid the current needs of the epidemic outbreak.[13–15]

In clinical methodology, the emerging mutations and the evolution of SARS-CoV-2 isolates are determined by DNA sequencing of bronchoalveolar lavage fluid (BALF) samples.[6,16] These BALF samples come in the form of nasopharyngeal swabs or sputum samples, and the viral nucleic acid detection is performed by reverse transcription-polymerase chain

G. Kabay, A. Altay, C. Dincer
FIT Freiburg Center for Interactive Materials
and Bioinspired Technologies
University of Freiburg
79110 Freiburg, Germany
E-mail: dincer@imtek.de
G. Kabay, A. Altay, C. Dincer
Department of Microsystems Engineering - IMTEK
University of Freiburg
79110 Freiburg, Germany

The ORCID identification number(s) for the author(s) of this article can be found under https://doi.org/10.1002/adma.202201085.

G. Kabay
Institute of Functional Interfaces - IFG
Karlsruhe Institute of Technology
76344 Karlsruhe, Germany
J. DeCastro, K. Smith, H.-W. Lu, A. M. Capossela, M. Moarefian, K. Aran
The Claremont Colleges
Keck Graduate Institute
Claremont, CA 91711, USA
E-mail: kiana_aran@kgi.edu
K. Aran
Cardea Bio Inc.
San Diego, CA 92121, USA

reaction (RT-PCR).[17,18] By amplifying the viral gene sequences to approximately a single-molecule level sensitivity, RT-PCR is considered the gold standard for any pathogen detection.[18] Compared to the next-generation sequencing technology,[19] RT-PCR-based techniques offer cheaper and applicable detection with a shortened response time down to 2 h.[20] However, several downsides also exist: i) requirement for a constant reagent supplement such as primers and polymerase enzymes to be performed, ii) highly specialized equipment used for testing requires complicated handling and present at high costs, iii) trained personnel for sample collection, preparation and analysis are required, iv) furthermore, considering the high demand for testing during an outbreak, the number of tests performed remain limited by the given capacity of central laboratories and the number of regulatory-approved (multiplexed) PCR assays,[21] v) transportation of samples from the testing facility to the central laboratory is time-consuming, error-prone (due to a possible contamination) and costly, hampering immediate isolation of the infected persons and thus, prompt suppression of the outbreak, vi) false positive/negative results due to wrong sample collection, issues related to isothermal amplification employed, possible denatured/dead genetic material of the virus, potential cross-reactivity with other viruses and the genetic variances between patients,[22] vii) manual reporting of the test results and their transfer and distribution to a digital database increases the susceptibility to human error and makes accurate bio surveillance, case reporting, and decision support more complex.[23]

Notwithstanding the recent advances in RT-PCR testing,[17,18] it only enables the identification of active carriers within a limited time frame. For example, in COVID-19 patients, the SARS-CoV-2 pathogen is detectable during its acute infection phase, which corresponds to 2–3 days after the onset of symptoms. Yet, it remains detectable until 14 days postsymptom onset, placing a temporal limitation on the efforts of diagnosing convalescent individuals.[10,18] Identification of the recovering patients, testing the efficacy of developed vaccines and therapies against viral infections are also critical. These allow a more comprehensive understanding of the immunity features against re-infection, estimate how the virus spreads over time, evaluate the virus's geographical distribution,[12,24] and are found in the form of immunology or serology assays that require the collected patient blood samples.

The humoral immunity features can be studied by screening the primary antibody immunoglobulin M (IgM) and secondary antibodies, such as immunoglobulin G (IgG) or immunoglobulin A (IgA). While IgM detection is preferred when rapid information (around 15 min) about possible ongoing infections needs to be assessed,[25] acquired immunity is determined using a neutralization assay to screen the number of anti-SARS-CoV-2 IgG levels diminishing promptly. On the other hand, IgAs, which protect mucosal surfaces against pathogens by neutralizing respiratory viruses or obstructing their attachment to epithelial cells, are shown to be more effective in virus neutralization than IgGs.[26] Typically, the detectable levels of neutralizing antibodies start declining three months postinfection, especially for wild and asymptomatic cases of COVID-19. However, the same is true for seasonal coronaviruses (sCoVs),[27] which may yield ambiguity in understanding the source of IgG, IgA, and IgM levels present in neutralization assays.

The most significant serological assays, based on chemiluminescent assays,[28] enzyme-linked immunosorbent assays (ELISA),[29] and lateral flow immunoassays (LFA),[30] are presently in use for determining immunoglobulin generation as a function of the adaptive immune response upon viral infection.[31,32] Among them, due to their low-cost, instrument-free, and easy-to-use nature, LFAs, in the form of rapid antigen tests using virus-specific biorecognition elements (like antibodies), are also highly favorable for on-site virus detection to control infectious disease spread to a certain extent.[33] All of the assays explained above are informative methods for rapidly identifying the current and previous exposures to a particular virus while also specifying the extent of infection.[27] However, their low accuracy, sensitivity, and specificity due to cross-reactivity with similar pathogens are restraining. Consequently, existing direct antigen tests and serological assays cannot substitute RT-PCR testing but are rather suitable as complementary diagnostic tools.[27,34]

These limiting factors, coupled with supply chain concerns and inconsistencies between the test results, led to alternating approaches such as biosensors, which can overcome the drawbacks of the conventional diagnostic methods for viral infectious diseases. From this standpoint, biosensors offer many promising features: i) low costs, ii) rapid, simultaneous, and susceptible detection of various analytes, iii) short turnaround times, iv) high specificity and selectivity, v) adaptability for on-site (even wearable) testing, continuous monitoring, and multiplexed detection, and vi) integrability for simultaneous data transfer to a central or distributed database.[34]

In this review, we shortly introduce the fundamentals of biosensors, followed by a survey of the state-of-the-art biosensing devices for detecting viral pathogens and/or associated (like serological and inflammation) biomarkers. Herein, we thoroughly discuss the advantages and drawbacks of each strategy. Later, we share our vision on next-generation biosensing technologies along with advanced materials and their use to detect viruses or other viral pathogen-associated biomarkers to control and combat such pandemics caused by viral infectious diseases in the future.

2. Designing Biosensors

A biosensor mainly consists of the following four elements (**Figure 1**): i) a bioreceptor, which is a molecule (either natural, synthetic, or bioinspired) with a high binding affinity toward a specific substance (i.e., target/analyte), enabling its biorecognition, ii) a transducer to convert this biorecognition event into a measurable signal, iii) an electronic circuit for signal processing and data evaluation (preferably, also for data transfer), and iv) a display element translating the output signal to predefined forms (numeric, visual, or illustration).[35,36]

In addition, biosensors may also include a sample preparation unit that allows on-site processing of samples straightforwardly.[37,38] Therefore, it is crucial to consider the types of biofluids to be analyzed for a specific target when designing a biosensor. For example, saliva and sputum are ideal candidates as biofluids for the COVID-19 diagnostics since the SARS-CoV-2 virus is transmitted through respiratory airways and mucosal
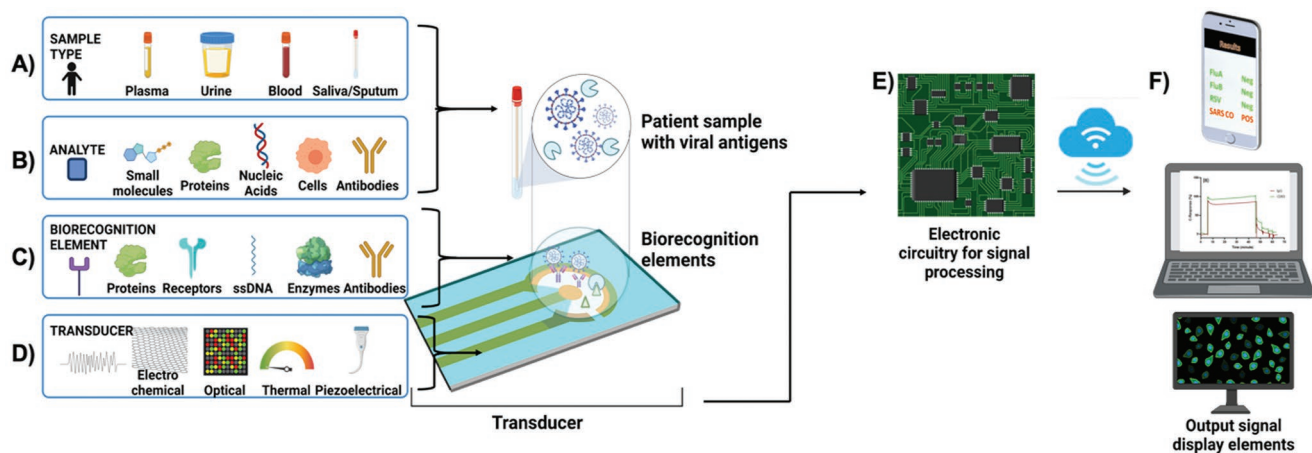
Figure 1. Schematic representation of a biosensor including all elements: A) Several sample types, including biofluids, such as plasma, urine, blood, or saliva/sputum for the analysis. B) Various analytes that may be targeted for diagnoses, such as small molecules, proteins, nucleic acids, cells, and antibodies. C) Surface modification with biorecognition elements like proteins, receptors, ssDNA, enzymes, and antibodies. D) Signal conversion of biochemical interactions to electronic readout with a transducer. E) Electronic circuitry for signal processing, analysis, and transmission. F) Display of results. All images within this figure are adapted with permission from Biorender.com with a paid academic subscription.

tissue. In the case of immune response detection via serological assays, blood-based samples such as whole blood, plasma, or serum are more favorable.

2.1. Substrate Materials

Biosensors in terms of their substrate material could be categorized as i) conventional materials for micro/nanosystems technology (like silicon, glass, ceramics, metals, and carbon-based materials), ii) synthetic polymers (such as elastomers, thermosets, and thermoplastics), iii) cellulose-based materials (including nitrocellulose and paper) and iv) hybrid materials to address deficiencies of single-material systems.[14]

Conventional micro/nanotechnology materials show excellent material characteristics, yet because of their stiff nature, stretchability can only be achieved by geometrical modifications. Even though cleanroom facilities and complex manufacturing techniques are required, their high cost could be overlooked by the established methods for mass production. On the other hand, synthetic polymers are mainly compelling because of their low cost and wide range of varieties offering distinct material properties. For example, poly(dimethylsiloxane) (PDMS) has enhanced elasticity and porosity than conventional substrates such as glass or silicon. Therefore, it is preferred especially for wearables and for prototyping microfluidic devices. An epoxy-based photoresist may be used to construct biosensors, such as a bisphenol-A novolac epoxy (SU-8), which offers excellent chemical stability, high aspect ratios, and biomolecule immobilization capability via adsorption. However, because SU-8 is expensive, its application in biosensors has been restrictive (mainly as isolation material, although it is also possible to create 3D microfluidics). In this regard, cellulose-based materials have become prominent since they are inexpensive, flexible, and biodegradable. Even though cellulose-based materials support the fabrication of microfluidic structures and their integration into wearable systems, fabricating controlled patterns at small scales (within micro or nanoscale) is challenging. To achieve augmented performance at a low cost, hybrid materials, usually created from the combination of polymers and other materials, are used. The composition of the hybrid materials depends on the design requirements of the biosensors.[39]

2.2. Transduction Methods

Methods for signal transduction in biosensors can be sorted into five categories: electrochemical, optical, microgravimetric, magnetic, and thermal detection.[40] Electrochemical biosensors are used widely because of their high sensitivity, fast turnaround times, miniaturization capabilities, and facile mass production at low costs.[41] Besides, optical biosensors are also extensively employed due to their enhanced sensitivity, robustness, and rapid detection.[42] For example, an optical method, surface plasmon resonance (SPR), offers sensitive detection of biomolecules without any labeling. However, the bulky and costly instrumentation of the current SPR devices is still an obstacle to the commercialization of this technology.[43]

On the other hand, microgravimetric biosensors, based in quartz crystal microbalance (QCM)[44] or surface acoustic wave (SAW),[45,46] detect changes in mass employing piezoelectric materials as transducers and thus, enable the highly sensitive detection of analytes in different environments (liquid, air, or vacuum). However, their capability for on-site testing and detection in complex biofluids are limited. With the advancements in magnetic biosensors (for example, giant magnetoresistance sensors), it is possible to achieve a rapid and real-time quantification of biomolecules by using magnetic nanoparticles (NPs), which lead to a change in the electrical resistance of the sensor upon binding to its surface.[47] Lastly, thermal biosensors are rarely employed for on-site applications due to the considerable influence of environmental temperature fluctuations on the results obtained. Thus, they are used for monitoring

**ADVANCED
SCIENCE NEWS**

www.advancedsciencenews.com

**ADVANCED
MATERIALS**

www.advmat.de

clinical and industrial processes under defined measurement conditions.[48] To reach the gold standards set by well-established methods like RT-PCR and serology immunoassays and to overcome the drawbacks of the different signal transduction methods, multimodal detection where at least two modes of detection are simultaneously employed (for example, optical-electrochemical detection) has been increasingly employed in biosensing. Although multimodal analysis increases complexity and production costs, it also elevates sensitivity, selectivity, and reproducibility.[14]

2.3. Surface Modification and Signal Amplification Strategies

The advances in nanoscience and nanotechnology have reinforced the development of unique nanomaterials, including monolithic and hybrid architectures such as photon-up conversion NPs (for example, lanthanide-doped nanocrystals).[49] They can be used as i) substrate materials, ii) labels in bioassays, iii) amplification tools, and iv) bulk/surface modifiers in biosensors.[14] The conventional nanomaterials employed are metals[50,51] (for example, platinum (Pt), gold (Au), silver (Ag) and magnetic nanoparticles, and quantum dots)—mainly due to their plasmonic (in the case of optical sensors) or electrocatalytic properties (for electrochemical sensors)—and carbon-based[51,52] (such as carbon nanotubes, graphene).

Since biosensors rely on the detection of biological recognition events on the sensor surface, the application of nanomaterials or various coatings for surface modification of biosensors results in signal enhancement that can improve sensitivity and selectivity, upon many other metrics: i) to increase biocompatibility and ii) conductivity, iii) to reduce biofouling, and iv) to enhance the immobilization of bioreceptors. So far, several surface modification techniques, including self-assembled monolayers (SAMs), monolithic or hybrid nanoparticles, electrodeposition of polymers/nanomaterials, and metal-organic frameworks (MOFs),[53] have been used. Although even single-molecule detection could be achieved using nanomaterials and/or coatings, further developments are necessary to eliminate their complexity and high cost for industrial applications.[54]

2.4. Biorecognition Elements

Bioreceptors are mainly classified as natural and artificial.[55–57] Natural biorecognition elements include nucleic acids, antibodies, enzymes, whole cells, etc., originate from living organisms and are harvested in laboratories. They are precise and cost-effective in the case of small-scale production. However, the large-scale production of natural bioreceptors is disadvantageous due to their high production costs and difficulties for scaling up.[14] Artificial bioreceptors, on the other hand, are either fully/partially synthesized or engineered from natural biorecognition elements.[57,58] They primarily consist of aptamers, molecularly imprinted polymers (MIPs), and recombinant natural bioreceptors (like antibody fragments). Artificial biorecognition elements offer a more stable solution for creating low-cost biosensors on a large scale when compared to natural bioreceptors. Yet, they require resource-intensive and time-consuming initial development, including multiple steps for their design, characterization, and optimization.[58,59]

2.5. Sample Preparation

For the diagnosis of viral diseases and the body response upon an infection, a great variety of sample types, including swabs, sputum, saliva, urine, stool, tissue, and blood-based specimens, exists. Herein, a proper and standardized sample collection (i.e., sampling) and preparation play a crucial role in obtaining accurate and reproducible test results.

After a sample is collected from a patient, it usually needs to undergo several preparation steps—dependent on the sample type and the analyte—before analysis. Liquid samples such as whole blood, plasma, saliva, and swab or sputum specimen are mainly preferred for testing infectious diseases-related parameters. For example, dilution or filtration is necessary for whole blood samples due to their surrounding complex matrix. Besides, depending on the analyte, additional processing steps such as centrifugation, precipitation, and deproteinization may have to be performed before testing specimens that exist in complex matrices, such as whole blood, serum, or plasma. On the other hand, sputum and throat, nasal or nasopharyngeal (gold standard for respiratory diseases) swab samples should be collected only with sterilized swabs, consisting of a plastic shaft along with a synthetic tip made of nylon, Dacron, rayon, or polyurethane, and having either a flocked or foam structure.[60,61] Upon sampling, the swab should be resuspended in either a viral transport medium or an elution/lysis buffer. The swab material and form should be carefully studied depending on the target type (nucleic acids or proteins) since they greatly influence the collection and release efficiency of the sample. Additional pre-treatment of the sample may be necessary for saliva analysis, like including protease inhibitors to decrease protein degradation. In the case of urine-based diagnostics, in addition to filtration due to high volume, pH adjustment also becomes necessary because of the wide range of pH values found in these samples.

On the other hand, more complex sample processing is necessary for solid samples, including stool and tissue.[62] Stool specimen, for example, requires intensive off-chip sample preparation, including vortexing, centrifugation, and filtration because of the presence of high concentrations of bile.[61] Additionally, complex matrices such as wastewater and soil, which could be analyzed for virus detection in environmental monitoring and risk evaluation during a pandemic, also require centrifugation, solid-phase extraction, and/or enrichment techniques, all demanding a complicated setup.[63]

For indirect pathogen detection, molecular diagnostics of viral genetic material needs extensive sample preparation to extract genetic material (i.e., nucleic acids) and subsequent isothermal amplification of these nucleic acids. First, unwanted cellular chaff might cause contamination of nucleic acid samples; therefore, a purification process becomes necessary. Second, the extraction of RNA/DNA is highly laborious and time consuming. Several proper nucleic acid extraction procedures include cell lysis, nucleic acid isolation from biological matrices (inactivation of cellular nucleases), and chemical

inhibitor elimination.[63] Accompanying extraction procedures, ultrafiltration by a membrane, and water drying with hydrophilic gel methods may be used to concentrate the nucleic acids in the sample.[61]

Because of the complexity of many procedures involving sample collection and preparation, diagnostic devices are susceptible to human errors and contamination risk. To overcome these issues, "sample-in, answer-out" biosensors with an integrated and fully automated sample preparation unit have been recently developed.[37] However, although these platforms offer rapid and quantitative analysis by directly processing patient specimens, their on-site testing capability is still limited due to their bulky size.[64]

2.6. Signal Analysis and Data Acquisition

Upon visualization of the biorecognition event by the transducer, the signal is transferred to the complex circuitry for signal processing, including converting from analog to digital format and signal amplification. This signal is then quantified by a (preferably integrated) display unit.[35] As signal varies, corresponding changes in noise may affect sensor performance. The signal-to-noise ratio (SNR) should be evaluated to quantify this effect.[65] Accordingly, a circuitry employing lock-in amplifiers, passive switches, capacitors, and filters could be designed to eliminate unwanted harmonics, lower power consumption, and thus, improve SNR.[66]

The integration of smart devices used in our daily lives like smartphones to biosensors, especially for point-of-care (POC) diagnostics, eliminates sophisticated hardware requirements for signal readout and analysis, as well as data transmission. For instance, the cameras of smartphones could be used to analyze optical signals, which can be later evaluated via an app.[13,67,68] Additionally, Internet-of-Things (IoT) integration to biosensing technologies would enable wireless data transfer and exchange between multiple smart devices and cloud-based servers.[69,70] Indeed, further advancements could be achieved with decentralization, enhancing data security by eliminating third parties (i.e., centralized laboratories and institutions).[71]

3. Biosensors for the Detection of Viral Infections

The measurement strategies used for the diagnosis of viral infections are categorized as i) direct pathogen detection (viral surface proteins or the virus itself),[13,72,73] ii) recognizing pathogen-associated viral genetic material such as nucleic acids (either viral RNA or DNA),[34,72–77] or iii) detecting the biomarkers that are present as a result of the specific host immune response, including antibodies,[34,72–77] proinflammatory cytokines and chemokines.[78,79]

3.1. Biosensors for Direct Pathogen Detection

Direct pathogen measurement is performed exclusively through antibody–antigen interaction[34,72–77] by targeting the virus-specific proteins[13,72,73] (nucleocapsid, surface, or transmembrane proteins) of a target pathogen. LFAs are routinely used for the (semi-)quantitative or qualitative detection of various analytes in clinical settings due to their low cost, easy applicability, and short turnaround times (5–30 min). Depending on the recognition elements used, LFAs can be grouped as lateral flow immunoassays (LFIAs) and nucleic acid LFAs (NALFA). In LFIAs, antibodies are employed as bioreceptors to gauge analytes, including proteins, antigens, and hormones, whereas, with NALFA, amplicons formed during the PCR are identified. In brief, LFAs consist of a conjugation pad, which has antibodies temporarily fixed to the surface.[30] A mixed sample is then placed sample pad which directs sample flow to the conjugation pad where the conjugated antibodies bind the analyte (or antigen) of interest. The analyte–antibody mix subsequently migrates along a membrane by capillary flow across test and control strips. These strips are coated with antibodies detecting the analyte of interest, and a positive test is confirmed by a color change in control and test lines.[30,80,81]

In contrast, biosensors for direct pathogen detection offer a straightforward methodology with a more applicable setup that reduces the error sources of the whole procedure.[34,82] In detail, when biosensors are utilized for the direct detection of viral pathogens, the interaction between the viral antigen-specific proteins and the proper capture biomolecules (for example, antibodies, surface proteins, or aptamers) is realized by screening the changes (in mass, optical or electrical signals) on the sensor surface. The virions of RNA viruses, including coronavirus and nidoviruses, are enveloped and take a form that contains four essential structural proteins: the spike (S) protein, which governs binding to host cell receptors and virus entry into cells; the membrane (M) protein; the envelope (E) protein, which mediates virion budding; and the nucleocapsid (N) protein, which together with genomic RNA constitutes the nucleocapsid and has an essential role in viral pathogenesis and replication.[73,83–85]

For instance, a field-effect transistor (FET)-based biosensor for directly gauging the SARS-CoV-2 was realized using an antibody against SARS-CoV-2 S protein immobilized on the graphene sheets of the gate.[85] The biosensor developed could detect SARS-CoV-2 viruses in clinical serum samples in real time, deprived of any pretreatment or preparation steps (**Figure 2**). Although the sensor performance reported is comparable with the standard ELISA tests, the universal transport medium used to store nasal swab samples caused a high noise signal. Indeed, the fabrication time (more than one day) and the multiple stages used to functionalize the biosensor surface limit its scalability. The results imply that different materials or engineering approaches should be implemented to reduce noise, ease their production, and improve the detection performance of such FET-based biosensors.

N protein is more predominantly present in various clinical samples such as sera, nasopharyngeal aspirate, throat wash samples, and urine, even at the early infection period.[73] Thus, utilizing N protein as a biomarker has shown to be an effective strategy for the early screening and identification of the patients infected by coronavirus variants, including SARS-CoV, MERS-CoV, SARS-CoV-2.

N protein detection has been accomplished by using variations of the SPR method to detect changes in localized waves
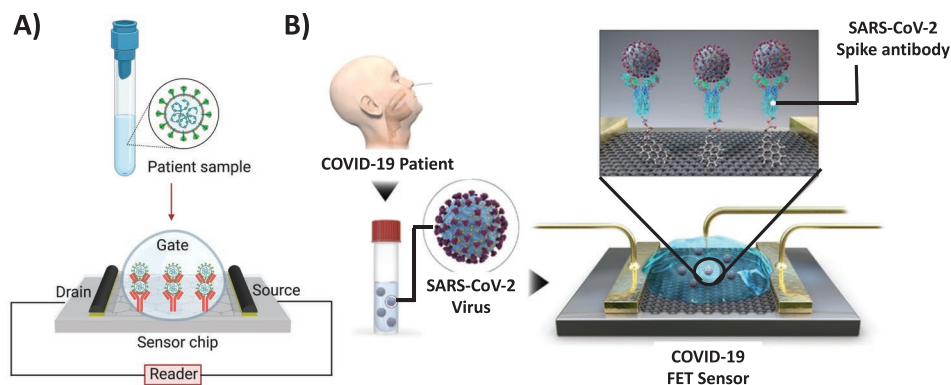
Figure 2. Field-effect transistors for direct pathogen detection. A) Schematics of direct viral detection using a field-effect transistor (FET)-based biosensor. The sensor surface is functionalized with capture biomolecules (here, antibodies). After introducing the patient sample, viral particles in the solution bind to the capture antibodies immobilized on the sensor surface and cause a measurable change which can be gauged via channel current and/or gate capacitance. All images within this figure are adapted with permission from Biorender.com with a paid academic subscription. B) Rapid detection of SARS-CoV-2 in human nasopharyngeal swabs using FET biosensors. The graphene-coated FET surface is functionalized explicitly with antibodies against the S protein of SARS-CoV-2 to measure the whole virus directly. Figures are adapted with permission.[85] Copyright 2020, American Chemical Society.

that go through the device (called surface plasmon oscillations) and react to refractive index changes along the gold surface of the sensor caused by the binding of biomolecules.[86,87] Recently, the detection of N protein in serum samples was achieved using a localized surface plasmon resonance (LSPR) coupled fluorescence fiber-optic biosensor.[72] This study utilizes sandwich immunoassay configuration to detect N protein of SARS-CoV, suggesting a comparable sensitivity and specificity to the conventional immunoassay setup conducted in parallel. Accordingly, it can be further enhanced by integrating chip-based assays to diagnose several diseases in the clinic. In another study, a label-free biosensor based on an optofluidic nanoplasmonic sensor was developed for proof-of-concept detection of RNA originated Ebola and DNA originated vaccinia virus in cultured cell samples.[88] The biosensor proposed is promising due to its performance for direct virus detection and adaptability for integration into a multiplexed format. However, analysis of real samples should be further carried out before deciding its eligibility for clinical use.

As previously mentioned, SPR detects the shifts in surface plasmon resonance upon biomolecule binding.[86,87] By monitoring these changes, antibody–antigen interaction can be visualized without any labeling in real time, making such sensors a decent candidate for on-site testing of viral infections.[86,89] Applying this approach, an SPR-based biosensor was established to detect SARS-CoV viruses targeting its E protein regions.[89] To form the biorecognition layer, a fusion protein consisting of a gold binding polypeptide (GBP) and an E protein was designed then self-immobilized (due to the thiol affinity of the GBP) to the Au chip surface in the absence of further chemical functionalization. The self-formed biorecognition layer could rapidly and precisely sense anti-E antibodies in physiological buffer solution. But an excess amount of cross-reactivity for other IgGs presence was observed. Also, the sensitivity was lacking due to the high detection limit obtained, and thus, it should be improved further for a clinical application.

In another optical variation, Au nanoparticles (AuNPs) were presented to detect the porcine reproductive and respiratory

virus (PRRSV), a positive-sense RNA virus found in pigs, in real time.[90] The optical response exerted by a conformationally changed antibody upon antigen binding in solution was detected using either fluorescent-labeled quantum dots or AuNPs combined with FRET. Although this study offers convenience for directly measuring isolated PRRSV samples, it is inapplicable, mainly due to the process variability and high batch-to-batch variation.[91] Therefore, an in-line fluidic setup should be developed for NP fabrication, functionalization, and validation before clinical utilization.[92,93] In a milestone study, the circulating N-antigens of the SARS disease were sensitively detected for the first time in sera specimens collected without any cross-reaction, utilizing a rapid antigen test along with a sandwich ELISA.[73] Hence, it can be effectively used in the clinic to identify the infected patients at the acute phase (the first 10 days after the symptoms are onset). In addition, the system developed is shown to be clinically applicable considering the high number of patient samples tested and the high specificity and selectivity obtained. Sample collection, dilution, and sensing elements could be integrated into a single module to enhance this system further.

As a feasible alternative, optofluidic biosensors, combining the simplicity, scalability, and versatility of microfluidics with the improved sensitivity and specificity of optics by integrating fluorescent probes,[94] lasers,[95,96] spectrometers,[97] or photonic crystals,[98] are emerging. Their superior features, such as label-free and high-throughput analyte detection, suitability for miniaturization, and multiplexing, are encouraging for real-time monitoring and on-site disease diagnosis. For example, in a proof-of-concept study, an optofluidic biosensor incorporating a whispering gallery mode (WGM) microlaser and suspended waveguide inside a microfluidic channel was established for Influenza A detection.[96] The total internal reflection of resonators improves the light–matter interactions at small volumes, while the large bandwidth of the laser provides single virus level detection with much higher sensitivity than passive resonators. In the meantime, the fluid handling incorporated with the microfluidic channels offered the portability expected

**ADVANCED
SCIENCE NEWS**
www.advancedsciencenews.com

**ADVANCED
MATERIALS**
www.advmat.de

from a POC device. However, because the technology described only tested for virus particles in the air and polystyrene NPs in water, its prosperous applicability when tested in human samples, remains a question. Therefore, further assay development and testing of this device with clinically relevant viral samples should be demonstrated to prove its potential utility in the clinic.

Another proof-of-concept study based on an optofluidic setup was carried out using 2D slab photonic crystal (PhC) sensors, termed 2-D slab-PhC, coupled with a waveguide.[99] The signal readout is performed via a laser and a photodetector. Here, the transmission spectra are obtained to detect the presence or absence of a single captured molecule inside the defect hole. The size of the defect hole provided a reduction of non-specific surface binding and interaction; however, the bulk of the assay's specificity was achieved through optical detection of virus-antibody capture on the surface of the microfluidic chamber. While the platform has yet to be tested on viral particles, it has shown promising preliminary results using functionalized and non-functionalized viral-sized latex particles. More research is needed to test the 2-D slab-PhC platform with clinical viral samples and further evaluate specificity and sensitivity. This technology detected viral simulants underflow of liquid and air, which shows its potential within airborne or fluid-based pathogens. Current temperature limitations due to the silicon PhC sensors and the extended surface functionalization and handling times, currently inhibit the use of the platform in point-of-care settings.

Mass-sensitive biosensors that utilizes piezoelectricity effect to detect and quantify mass changes created on an electrode surface, mainly resonating quartz crystals, are another approach applied for the rapid detection of pathogens.[100] For instance, the use of such a platform was shown for measuring SARS-CoV in sputum samples after evaporating the virus-containing samples in the gas phase.[75] Due to the piezoelectric effect, the binding of the SARS-CoV virus on the electrode surface caused a frequency shift in crystal resonance frequency; therefore, calculating this frequency change, the loaded mass, hence, the virus concentration was quantified. Although this biosensor is reusable and offers a reproducible and specific detection of SARS-CoV, contamination and infection risks during sample preparation must be carefully evaluated before further adaptation to clinical applications.

Despite the differences between the sensing methods discussed thus far, one universal condition would be imperative in further developing the field: multiplexing (i.e., multianalyte detection) capabilities. Multiplexing is especially important to differentiate between seasonal allergies, common cold, flu, and other viral detection, especially when the initial symptoms (such as respiratory problems, fever, etc.) for those may appear similar; however, their treatments vastly differ. Typically, multiplexing can offer higher accuracy through the simultaneous detection of various pathogens while also providing a potentially simpler workflow and less risk of sample contamination.[101] Furthermore, the throughput of testing increases, proving that multiplexing is a critical approach for improving the cost and time efficiency of POC diagnostics.[102] For example, there are extensive efforts for multiplexing the detection of Influenza viruses simultaneously with SARS-CoV-2. Such technologies

have recently been approved for use under the Food and Drug Administration[103] and vary in complexity from simple, at-home tests requiring little to no training and a low risk for an incorrect result to moderate-higher complexities.

In a typical example of multiplexing, the immunocomplex formation was realized in conductance change, and virus detection was evaluated in real time using a silicon nanowire–Au array modified FET.[76] The Influenza A virus could be selectively detected amongst structurally similar adenovirus and paramyxovirus through electrical measurements and optical imaging. Due to high sensitivity, selectivity, and simple instrumentation, the proposed multiplexed platform shows an excellent promise for adaptation to clinical applications. However, further studies should be exploited to enhance the multiplexed detection performance of the system proposed by testing multiple viruses and their variants simultaneously. In addition, large-scale adaptation should be evaluated before deciding clinical transfer. Another study based on an optofluidic LOC device was established to detect viral epitopes of SARS-CoV-2 and Flu A responsible for COVID-19 and Influenza diseases, respectively.[94] Here, an optical analysis unit is incorporated with an amplification-free differential diagnostic setup based on biophotonic assay antiresonant reflecting optical waveguides (ARROW). Briefly, streptavidin-coated beads were functionalized with biotin-labeled SARS-CoV-2 or Flu-A antibodies, while a photocleavable spacer gives fluorescent reporting upon detection. This optofluidic chip allows single-antigen detection in a multiplexed mode by intersecting the analyte signal, and a multimode interference (MMI) excitation waveguide. The MMI platform supports multiple modes, or the standing wave state of an excitation wave[104] that have different propagation constants. MMI presents a wide waveguide phenomenon, which supports several waveguide modes for multianalyte detection. Although only two different fluorescent labels were used for the differential diagnostics of the SARS-CoV-2 and Flu A viruses, the platform itself can be configured for up to seven multiplexed antigens with variations to the MMI layout. While this system shows promising results using negative PCR tested nasal swabs spiked with the respective pathogens, the number of steps in the assay and the complex and precise instrumentation needed to perform differential diagnostics significantly limits its clinical utility. However, the high level of sensitivity and specificity along with an amplification-free protocol are promising features of this platform; therefore, its clinical adaption is possible after pointing out these issues.

Alternatively, the multiplexing paradigm by wavelength division would allow differentiative identification and detection of a single virus; their subtypes and possible mutations can be identified through trapping under flow conditions. With this motivation, optical wavelength division (405–745 nm) was used to establish wavelength-dependent spot patterns on an ARROW optofluidic chip that enhances its multiplexing capacity to concurrently detect fluorescent-labeled Influenza A subtypes (like H1N1, H2N2, H3N2).[105] Although the reported performance with a femtomolar level is sufficient for clinical applications, its feasibility with patient samples should be tested prior to its adaptation as a diagnostic tool. In case of on-site testing, a miniaturization of the measurement instrumentation as well as a re-evaluation of microfluidic integration to achieve better

sample processing and distribution for increased efficiency are required.

A similar multiplexed optofluidic approach enhanced by trapping functions to visualize single viral molecules was successfully demonstrated for the adenovirus detection.[106] Herein, a sandwich assay is employed, where polystyrene beads coupled with adenovirus antibodies were first incubated with the sample and then, the complex was labeled with signaling antibodies with quantum dots. After the immunolabeling protocol, the solution is flown through the optofluidic chip, in which a nanowaveguide-paired array generates potential wells, trapping the bead–virus complexes at constant trapping positions. Due to the small size of the adenoviruses, multiple viruses could be bound to a single bead. The quantification of the number of viral particles per bead was achieved by the individual fluorescence readings of each quantum dot. As more complexes are trapped and the fluorescence is continuously quantified, a plateau is reached, signifying that all wells are filled. This platform offers many benefits, including the need for a small sample volume, and high sensitivity (allowing an amplification-free detection) and specificity thanks to the sandwich assay used. However, it is currently limited by the geometry of a 16-nanowaveguide-pair chip, which diminishes trapping capability down to 130 particles. Nevertheless, increasing the number of nano-waveguide pairs or expanding the width of the microchannel for entrapment can expand the trapping capabilities.

Following a similar multiplexing approach, a magnetoresistance biosensor consisting of 64 arrays decorated with magnetic nanoparticles (MNPs), was introduced for real-time detection of the Influenza uenza A virus.[77] A sandwich immunoassay was performed to detect and continuously monitor viral N proteins present in nasal swabs, suggesting a comparable performance with the ELISA counterpart. This biosensing platform is up-and-coming for large-scale adaptation to achieve combinatorial and detection of multiple pathogens in a single step. However, extended sample preparation and biosensor fabrication steps are challenging.

Another study introduced a laser-engraved graphene immunosensor integrated with a wireless data transfer module as a portable COVID-19 at-home testing device, RapidPlex.[107] SARS-CoV-2 N protein, IgG/IgM, and C-reactive protein (CRP) can be simultaneously quantified using this system. The multiplexed detection of these analytes simultaneously provides information on the active infection through N protein, the previous condition through IgG/IgM, and disease severity via CRP. These together facilitate the complete prognosis of COVID-19 patients. Incorporating this multiplexed platform with a mobile user interface allows data to be wirelessly transmitted to healthcare providers. Thus, this immunosensor not only delivers immediate sample-to-answer turnaround with high sensitivity and specificity by utilizing noninvasive body fluids such as serum and saliva. It also displays potential POC use through telemedicine for patient triage and remote monitoring. On the other hand, further progress can be made by incorporating an automated sample-handling process before full adoption for telemedicine and the POC distribution to build on these promising results.

Recently, an electrochemical biosensor, namely "RAPID," has been developed to detect the SARS-CoV-2 virus and its United Kingdom variant by examining patient saliva and

nasopharyngeal/oropharyngeal swab samples.[108] The RAPID sensor modification was achieved by drop-casting Nafion (1%) on working electrode surfaces of the screen-printed carbon electrodes to increase robustness, and interestingly, without sacrificing sensitivity. Electrochemical impedance spectroscopy (EIS) measurements were conducted to evaluate SARS-CoV-2 related S protein interaction with its receptor, angiotensin-converting enzyme 2 (ACE2), known to be downregulated upon coronaviruses' entry into cells. Due to displaying superior analytical performance than its peers, this rapid (4 min), low-cost, easily manufactured, and portable device proved its suitability for POC testing of the SARS-CoV-2 virus.

Other methods that employ different biorecognition elements for viral pathogen detection are based on molecularly imprinted polymers (MIPs),[98] cell-based membrane proteins,[13,110] and antibody mimic proteins.[111] MIPs are highly favorable as bioreceptors due to the tailor-made binding sites, which fully complement the template molecules in size, shape, and functional groups. Thanks to their high specificity, they can interact with the whole viral particle rather than just its receptor site, which is the norm in typical biosensing methods involving native antibodies.

For example, a pathogen detection platform based on MIP-modified quartz crystal microbalance (QCM) enabled selective detection of human rhinovirus (HRV) in suspension form.[112] A viral template was introduced to create a virus stamp that binds the subjected viruses. The surface engineered cavities enable studying the interaction between artificially designed recognition material and target pathogen by varying geometrical shape and surface chemistry (**Figure 3**). The intragroup and intergroup selectivity of the sensor experimented across
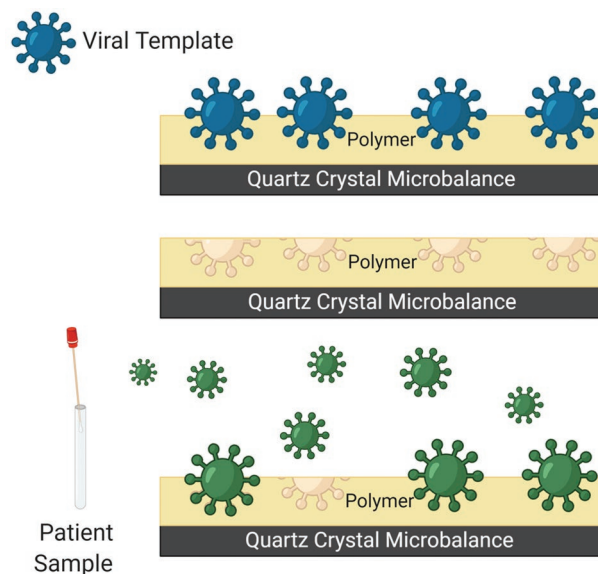
Figure 3. MIP-based label-free virus detection using quartz crystal microbalance. The polymer surface is "stamped" using a viral template that creates cavities in the polymer surface. After introduction with the patient sample, viral particles bind to the polymer cavities. These binding interactions are then detected by the quartz crystal microbalance. Such a biorecognition strategy of viruses could be also applied to other biosensing devices. All images within this figure are adapted with permission from Biorender.com with a paid academic subscription.

2201085 (8 of 30)

major/minor HRV serotypes (like HRV1A, HRV2, HRV14, and HRV16) and another type of picornavirus, foot-and-mouth disease virus (FMDV), respectively. Due to the sensitive and selective detection obtained, such a system is worthwhile mainly to evaluate the interaction mechanisms of pathogens and their serotypes with specifically engineered recognition materials. Biosensing technologies that use antibody-antigen binding interactions are limited by the availability of antibodies for newly occurring pathogens, artificial biorecognition elements like the MIPs can get around this hurdle.[98] However, integrating MIPs with QCM limits its mass production; hence, in the future, a further adaption of MIPs with different transduction (such as optical or electrochemical) methods that have better scale-up feasibility required for the clinical utility as well as promising capability for on-site testing. Advancing the MIP technology will allow distinct virus diagnosis, with limited or no interference, regardless of the group (minor or major) to which they belong or its subtypes/variants. For example, in the COVID-19 scenario, MIP-modified biosensors can selectively detect the SARS-CoV-2 virus amongst other coronaviruses that belong to the same family (MERS-CoV and SARS-CoV) and its variants[113] (SARS-CoV-2-α, -β) by manipulating artificially crafted pathogen-specific surface groups of the receptors.

Following an unconventional approach, the SARS-CoV-2 spike S1 antibodies were electroinserted into membrane-engineered cells, which were used to modify the surfaces of 8-array PDMS attached screen-printed Au electrodes.[13] Upon S protein binding to the membrane-bound receptors, the caused changes in the membrane potential and other bioelectric properties of the cell membrane were detected through a bioelectric recognition assay. Also, the hyperpolarization of the engineered cell membrane could be rapidly (within 3 min) identified without any pre-extraction, amplification, and cross-reactivity; also, the integrated readout interface enables real-time screening in a user-friendly manner. Although this proof-of-concept study shows its potential in pathogen detection, further clinical studies should be utilized to detect various analytes using multiple engineered cell membranes.

Transduction and amplification of the biorecognition events into an electrical readout directly affects the quality of the output signal, hence the sensor performance. Recently, bioelectronic transducers, namely organic electrochemical transistors (OECTs), have emerged as an alternative to solid-state electrolyte-gated transistors, mainly allowing for sensor surface biofunctionalization with nanobodies. Following this approach, the depletion-mode poly-(3,4-ethylendioxythiophen)-poly-(styrolsulfonat) (PEDOT-PSS) modified gated electrodes functionalized with green fluorescent protein-tagged nanobodies was established for pathogen detection.[114] The distinguishing performance of the sensor was shown over unprocessed SARS-COV-2, and MERS virus specimens both in buffer and saliva mediums, together with its modular and disposable format and rapid detection features imply its potential applicability for POC diagnostics. However, the simplified configuration of this device should be developed to increase its applicability by minimally trained personal in on-site settings. In another study, the recognition of the whole Hepatitis B virus and viral/antiviral components was achieved by utilizing engineered receptor-transduced cells that can express reporter and antiviral

molecules.[110] The mechano-transduction-based detection scheme was employed while converting ligand binding (input) into proteolytic release of the sequestered transcription factor, which enters the nucleus to express the desired genetic material as an output. Moreover, this platform reveals the capacity of engineered cellular biosensors not only for sensing but also to develop appropriate immunotherapies against viral infections through customized re-programming. For clinical adaptivity, appropriate signal amplification needs to be applied to decrease the long response time (currently around 24 h).

Although biosensors for direct pathogen detection offer various advantages over conventional immunoassays and are promising, most are still in their infancy. Hence, further efforts should be concerted to build integrated biosensing devices. **Figure 4** depicts some of the featured multiplexed and all-in-one technologies. Moreover, additional clinical and on-site studies using biosensors should be performed to prove their feasibility for use at the POC.

3.1.1. Aptasensors

Aptamers are single-stranded DNA or RNA oligonucleotides (with a length of 20–100 nucleotides) and can be employed as artificial bioreceptors. The aptamer sequence having high affinity and specificity to the target of interest is selected from a sequence pool containing different nucleotide variants through a high-flux screening method named "Systematic Evolution of Ligands by Exponential Enrichment (SELEX)."[115] After repetitively processing binding, washing, and amplification steps by SELEX, the resultant aptamer achieved optimum interaction with the target analyte of interest and was easily distinguished.[116,117]

Aptamers are frequently compared with antibodies due to their interaction with the analytes; therefore, they are known as "chemical or artificial antibodies."[117] However, they usually offer better performance than monoclonal antibodies when applied as a biorecognition element to build "aptasensors." The reasons behind their extensive usage in many applications, particularly for virus detection and treating viral infections, can be summarized as follows: i) reproducible and cost-effective chemical synthesis process, which does not require living organisms as raw materials; ii) easy selection procedure, which does not depend on a particular analyte, iii) due to the elimination of cross-reaction during SELEX, the resultant aptamers have high specificity between different virus genotypes, iv) high affinity and selectivity toward the target analyte; v) high thermal and chemical stability, vi) ease in modification and functionalization and labeling without loss of function, vii) nontoxicity and low immunogenicity.[115,117]

By coupling aptamers with several methods, including PCR and ELISA, improved sensitivity and selectivity could have been achieved.[117] For instance, an electrochemical aptasensor integrated with a sandwich-type enzyme-linked oligonucleotide assay (ELONA) was applied to selectively measure the inactivated Influenza A subtype (H1N1) among its variants (Influenza B, H7N9).[118] Using EIS, this study indicated that the standard ng-level sensitivity of the conventional ELONA was significantly improved to pg-level proposing a better performance.

**ADVANCED
SCIENCE NEWS**

www.advancedsciencenews.com

**ADVANCED
MATERIALS**

www.advmat.de
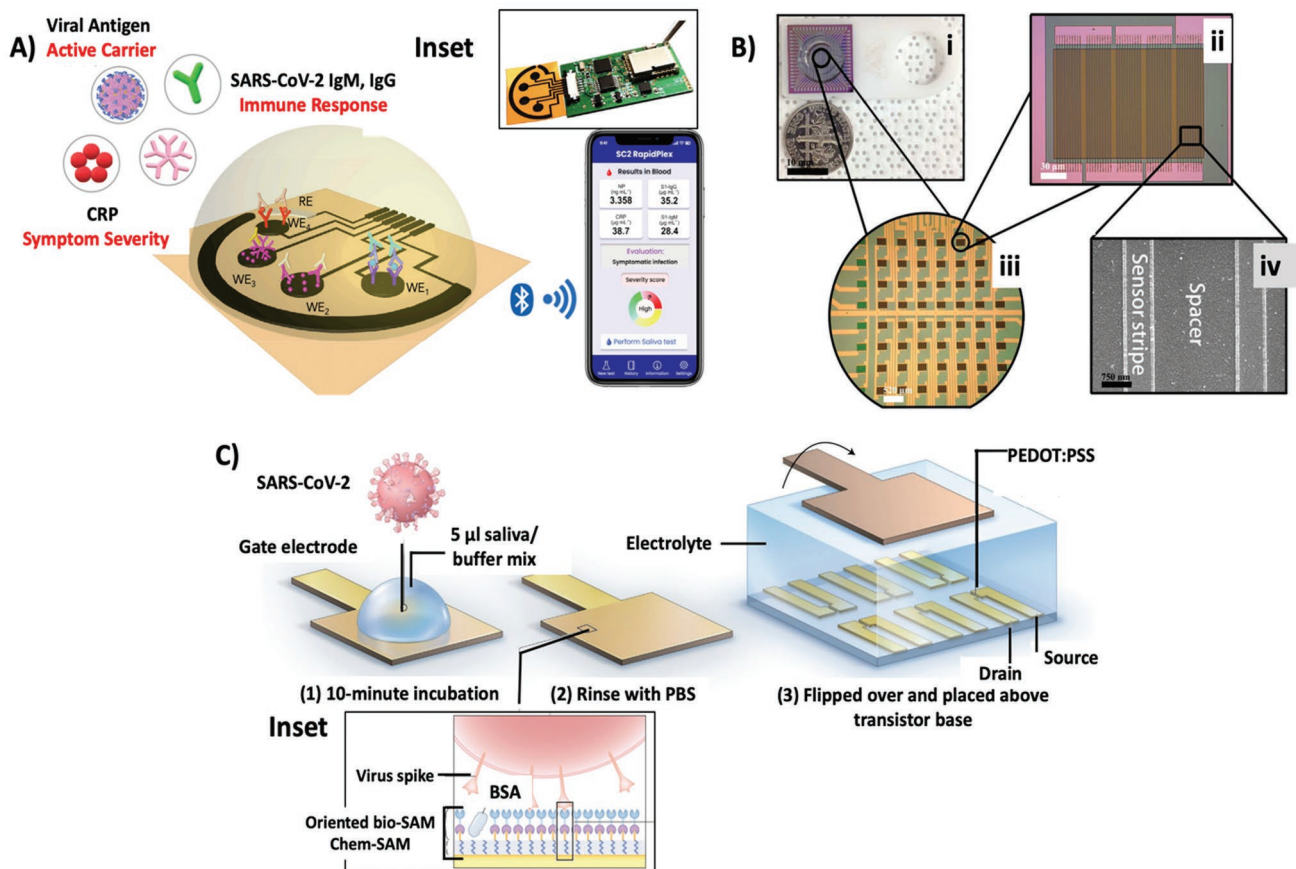
Figure 4. All-in-one viral detection biosensors. A) SARS-CoV-2 RapidPlex as a graphene-based multiplex sensing platform for SARS-CoV-2 viral antigens, immune responses, and C-reactive protein (CRP) that is associated with symptom severity with Bluetooth capabilities for telemedicine. Inset shows the complete device. Figures are reproduced with permission.[107] Copyright 2020, Elsevier Inc. B) Giant magnetoresistance (GMR)-based biosensor for detecting the Influenza A virus. (i) GMR fully functional chip with (ii) 8 × 8 sensor array that is functionalized with capture antibodies against IAV (iii) magnified portion of a GMR biosensor: Each GMR chip contains five GMR strip groups in series, and each strip group contains 10 GMR strips connected in parallel (iv) Specific sensor strips. Figures are reproduced with permission.[77] Copyright 2016, Frontiers Inc. C) Schematic of organic electrochemical transistors (OECTs) to detect COVID-19 and MERS antigens. A sample mixture of saliva and the binding buffer is introduced to the gate electrode. The electrode is flipped and mounted on top of the OECT channel for pathogen detection upon rinsing. The gate electrodes are functionalized with PEDOT: PSS for detection. The inset shows the molecular interactions of the viral S proteins to the oriented-SAM and chemical-SAM layers the electrodes are functionalized with. Figures are reproduced with permission.[114] Copyright 2021, under exclusive license to Springer Nature Limited.

Additionally, the effect of oligonucleotide probe density on signal performance was evaluated. In contrast to the sensitivity, the selectivity of the aptasensor was enhanced when decreasing probe density suggesting saturation of the sensor surface and steric hindrance, which plays an essential role in hybridization efficiency needs to be carefully optimized to ensure good performance. Besides enabling direct detection of a viral pathogen genome in one step (without any pretreatment stages), the utilization of inactivated viral DNA detection in this study presents a safe way for virus detection. Hence, it will guide further studies in overcoming biosafety issues during detection. However, testing with patient samples should be achieved to prove its POC applicability.

In another study, a similar strategy has been undertaken to differentiate the subtypes of Influenza A H1N1 virus from its variants (seasonal H1N1, H3N2, and 2009 H1N1) both by targeting recombinant Influenza A mini-hemagglutinin (mini-HA) protein (the stable stem region of HA) or the whole

H1N1 viruses.[119] The experimental protocol involves multiple rounds of SELEX with the mini-HA proteins to select the active conformation for the broad detection of Influenza A group 1 viruses. At the same time, the selection of H1N1-specific aptamers is followed by six rounds of SELEX with H1N1 viruses. An enzyme-linked aptamer assay was used to compare the binding behaviors of the PCR products after multiple rounds of being subjected to mini-HA and with H1N1 viruses. The ssDNA pools from each selection round were stored and amplified with biotinylated forward and reverse primers. In addition, developed aptamers were used as receptors instead of antibodies to build ITO/glass-based electrochemical aptasensor. The system was tested against six strains of H1N1 viruses, two strains of H3N2 viruses, adenovirus virus, Influenza B virus, and HA proteins of four different subtypes of Influenza A virus (H5N1, H1N2, H1N3, and H1N8). Although this study suggests a rapid, selective, and low-cost virus detection and subtyping tool relying on ssDNA aptamers, it is not

suitable yet for POC use due to limitations in standardization and complex procedure.

Although the methods summarized above provided enhanced sensitivity and specificity, most of them still require laborious devices to perform viral pathogen detection and cannot be applied to POC testing to detect multiple targets in a miniaturized device. Moreover, nucleic acid-based diagnostic probes authorized by microfluidic integration of plentiful processes such as aptamer selection, amplification, and multiplexed detection of various analytes by a single device would overcome the problems associated with the POC testing of target viral sequences.[116] Microfluidic-enhanced SELEX chips can hurdle this problem and are expected to become standards in the POC selection of aptamers and achieve hybridization reactions in a single device. For instance, by integrating an entire SELEX process (incubation, extraction, and amplification of nucleic acids) in a single microfluidic device, an aptasensor was introduced for Influenza testing (H1N1, H3N2, and Influenza B).[120] SELEX chip consisted of two PDMS layers on a glass substrate. After the aptamer selection, a magnetic bead assay was employed to demonstrate each virus's sensitive and selective detection. Such an approach suggests the applicability of microfluidic-empowered biosensors for POC detection of virus-specific aptamers that can be further improved with automated schemes and multiplexing. Furthermore, more collective efforts are needed to develop fully integrated/automated systems to detect viruses after the aptamer selection (**Table 1**).

3.2. Indirect Methods for the Detection of Viral Genetic Material

Nucleic acid (NA) testing is critical for determining the viral genome and promotes the early diagnosis of viruses. Indeed, detecting pathogens through identifying their unique genetic material enables obtaining more accurate information on disease-related features that vary due to genetic variances and mutations, screening patients, confirming suspected cases, and conducting virus surveillance.[121]

The earliest approaches for NA testing relied on the plate cultivation of pathogens.[122,123] Following, laborious cultivation-based assays could have been progressively replaced with polymerase chain reaction (PCR) technology. Briefly, PCR consists of DNA polymerase and DNA primers specific to the 3' ends of the sense and antisense strands of template DNA (the DNA strands available in samples of interest). DNA polymerase and the primers are employed to synthesize new strands of DNA complementary to the original template strand. After synthesis, several rounds of exponential amplification yield copies of the newly synthesized DNA (amplicons). These amplicons vary depending on the primer sequences and their complementary original nucleotide sequences.[124,125] PCR is essential for NA detection, given that in complex samples such as blood or saliva, the amount of viral DNA may be very little compared to host DNA. Fortunately, only viral DNA-specific primers are amplified with PCR method. Therefore, after a few rounds of amplification, the DNA concentration of the host will become negligible compared to the viral DNA, allowing the PCR to achieve selective and sensitive viral NA detection.

For coronaviruses, particularly in the COVID-19 scenario, quantitative reverse transcription-PCR (qRT-PCR) tests have been extensively performed, where first the target viral RNA is converted into a complementary DNA (cDNA), which is required for isothermal amplification.[126] To detect viral components, first, specific primers that can recognize the molecular targets secreted within the single-stranded RNA genome of the virus, such as open reading frame 1a/b or 8 (ORF1a/b or ORF8) regions, N-, S-, and E-genes, and RNA-dependent RNA polymerase (RdRP) need to be designed and tested.[127,128]

Although PCR technology has advantageous features, there are caveats to the technology pertinent to pathogen detection. For instance, the trace number of pathogens and their related genetic substance existing in collected specimens may result in false negatives, whereas the "inert" antibodies obtained from the recovered patient's samples may cause false positives and can be misleading while decision making. Furthermore, fundamentally, amplification of the NA product takes place during the exponential phase. Depending on the amount of accumulated product, self-annealing can happen, and thus, it makes endpoint quantification of viral pathogens potentially unreliable. In addition, i) sample collection and transportation-related issues (such as sampling error, denaturation of the sample while transporting), ii) the insufficient number of clinical facilities and complicated device setup and maintenance issues (including lack of clinical facilities and qualified personnel to perform an extensive number of tests promptly during a pandemic), iii) resource shortage and inadequate quality of reagents and extraction kits provided when high demand and supply gap are problematic.[129]

Therefore, to limit falsifying test results while testing a limited sample volume, one must obtain an intense signal output. All these aspects point out that potent NA detection methods empowered by biosensor technology are critical. Hence, we present biosensors incorporated with several nucleic acid testing platforms, mainly based on isothermal amplification-, clustered regularly interspaced short palindromic repeats (CRISPR)-, and nucleic acid-based assays (**Figure 5**).

3.2.1. Biosensors Combined with Isothermal Amplification

The conventional PCR technologies rely on temperature control instruments employed to achieve multiple temperature cycles during the amplification step of the nucleic acids. This problem was later solved by isothermal amplification methods, which enabled a simple and cost-efficient way for viral gene replication at a constant temperature by a water bath or a heating block.[130] Considering the working principle and the assay enhancing features, isothermal amplification approaches that have been extensively used in the virus genome diagnosis era can be categorized as following: rolling-circle amplification (RCA), loop-mediated isothermal amplification (LAMP), recombinase polymerase amplification (RPA), and nucleic acid sequence-based amplification (NASBA).[130,133]

The RCA-based assays amplify DNA or RNA primers forged to a circular small single-stranded DNA (ssDNA) template using DNA or RNA polymerases. In traditional RCA, bulky and laborious gel electrophoresis has been employed to detect

Table 1. Biosensors for direct pathogen detection (S1 protein: spike protein 1, N protein: nucleocapsid protein, Ab: antibodies, GNPs: gold nanoparticles, Ni: nickel, NPs: nanoparticles, HAV: Hepatitis A virus, GP: glycoprotein, GBPs: gold binding polypeptides, CRP: C-reactive protein, PBA: 1-pyrenebutyric acid, ACE2: angiotensin-converting-enzyme-2, AMPs: antibody mimic proteins, NWs: nanowires, MNPs: magnetic nanoparticles, TCID50: median tissue culture infectious dose, PFU: plaque-forming units, HRV: human rhinovirus, FMDV: foot and mouth disease virus, MIP: molecularly imprinted polymer, QCM: quartz crystal microbalance, MERS-CoV: Middle East Respiratory Syndrome-Coronavirus, CNTs: carbon nanotubes, Nbs: nanobodies, GFP: green fluorescence protein).

| Disease	Sample type	Signal transduction	Sensor/electrode material	Surface modification	Bioreceptor	Target	Sensitivity	Linear range	Turnaround time	Refs.
SARS-CoV-2	Isolated S-1 protein in buffer Nucleocapsid protein in buffer	Electrochemical	Au	PDMS membrane	Anti-S1 Ab	S1 protein	1 fg mL^{-1}	10^{-5}–10^3 ng mL^{-1}	3 min	[13]
SARS-CoV	SARS-CoV N protein in buffer Spiked SARS-CoV N protein in diluted human serum	Optical	Silica	GNPs	Anti-N-1 Ab Anti-N-2 Ab	N protein	1 pg mL^{-1}	0.1–10^3 pg mL^{-1}	2 min	[72]
SARS-CoV	Convalescent-phase sera	Optical	Western blot and ELISA	N/A	Anti- SARS-CoV Ab	N protein	50 pg mL^{-1}	0.1–3.2 ng mL^{-1}	17 h	[73]
HAV	Live HAV vaccine in buffer and diluted human serum	Optical	Polydopamine	SiO$_2$ NPs	PDA-coated virus-imprinted polymer	HAV	8.6×10^{-12} M	0.04×10-9 M	12 h	[74]
Influenza A	Whole IAV in buffer	Electrical, optical	Ni	Silicon NWs	Anti-Influenza A Ab	Influenza A	Single viral particle	0.6 - 4 µg mL^{-1}	>2 min	[76]
Influenza A	Whole IAV isolated buffer	Magnetic	Metal alloy	MNPs	Anti-Influenza A Ab	Influenza A NP	1.5×10^2 TCID50 mL^{-1}	0.3 - 10^5 TCID50 mL^{-1}	≈1 min	[77]
SARS-CoV-2	Cultured virus in media Virus in nasopharyngeal swab	Optical	Phosphate-buffered saline and clinical transport medium	Graphene sheets	Anti-S1 Ab	S1 protein	1.6×10 PFU mL^{-1} 2.42×10^2 copies mL^{-1}	1 fg mL^{-1} 0.1 pg mL^{-1}	≈11 min	[85]
Ebola Vaccinia virus	Vaccinia virus in media	Optical	Ti & Au	Protein A/G	Ab	Ebola GP Vaccinia GP	<10^5 PFU mL^{-1}	10^6–10^9 PFU mL^{-1}	30 min	[88]
SARS-CoV-2 Influenza A	PCR-negative spiked nasopharyngeal swab samples	Optical	MMI waveguide	Streptavidin reporters	Anti-SARS-CoV-2 N protein Anti-Influenza A antigen	SARS-CoV-2 N protein Influenza A antigen	30 ng mL^{-1}	N/A	45 s	[94]
Adenovirus	Adenovirus spiked buffer	Optical	Silicon nanowaveguide	Polystyrene NPs	Adenovirus antibody	Adenovirus antigen	13 particles µL^{-1}	N/A	2 h	[106]
SARS-CoV-2	Saliva Nasopharyngeal	Electrochemical	Carbon	Nafion	ACE2	SARS-CoV-2 S protein	1.39 pg mL^{-1}	0.1–100 ng mL^{-1}	4 min	[108]
SARS	N protein in the buffer solution	Electrical	Au	In$_2$O$_3$ NWs	AMPs	N protein	0.6×10^{-9} M	$0.6 - 10 \times 10^{-9}$ M	10 min	[111]
HRV FMDV	Whole virus in the suspension buffer	Microgravimetry	Au	MIP	Polyurethane MIPs	HRV FMDV	100 µg mL^{-1}	100 – 300 µg mL^{-1}		[112]
SARS-CoV-2 MERS-CoV	Saliva Serum	Electrochemical	Au	CNTs	Camelid-derived Nbs	SARS-CoV-2 S1 protein MERS-CoV S1 protein	1.2×10^{-21} M	0.25 mg mL^{-1}	10 min	[114]
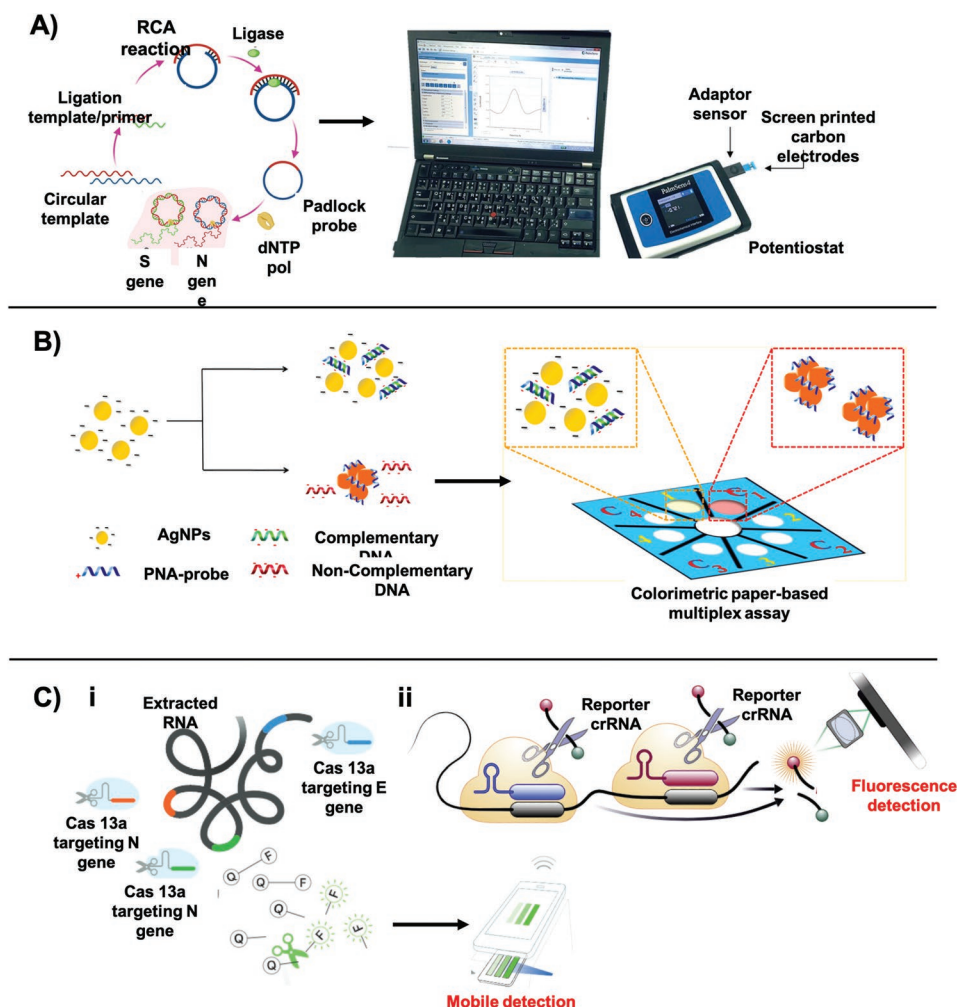
Figure 5. Indirect detection of viral genetic material using various techniques. A) An example of viral detection in conjunction with isothermal amplification methods: Rolling circle amplification (RCA) and electrochemical biosensor detection of SARS-CoV-2 N- and S-genes.[130] The multiplexed RCA reaction includes a sandwich hybridization of RCA amplicons onto probes with redox-active labels for detection via a potentiostat using pulse voltammetry. Figures are reproduced with permission.[128] Copyright 2021, Springer Nature Limited. B) An example of nucleic acid hybridization sensors for viral detection. Multiplexed paper-based colorimetric DNA sensor using peptide nucleic acid (PNA)-induced AgNP to detect MERS-CoV, MTB, and HPV oligonucleotides.[131] A pyrrolidinyl PNA probe functionalized to AgNP, after which binding MERS-CoV, MTB, and HPV DNA present a loss of aggregation in the nanoparticles and a colorimetric change. Figures are reproduced with permission.[129] Copyright 2017, American Chemical Society. C) An example of CRISPR-Cas associated techniques for viral detection.[132] Multiple CRISPR RNAs (crRNAs) were combined for the preamplification-free detection of SARS-CoV-2 RNA using Cas13a, simultaneously targeting N- and E-genes of SARS-CoV-2. Extracted RNA was easily detected under fluorescence reporting of crRNAs utilizing a mobile phone-based device. Figures are reproduced with permission.[130] Copyright 2020, Elsevier Inc.

and quantify the RCA amplicons and classify them depending on their geometrical differences.[134] On the other hand, electrochemical biosensors can be combined with an RCA assay to enhance its performance for the rapid detection of a trace amount of genetic material. For example, the N-, S-genes of the SARS-CoV-2 virus were measured by a single-step sandwich hybridization assay using a redox probe (methylene blue or acridine orange) tagged silica NPs.[130] With this method, the detection limit of targeted gene sequences could be decreased to 10^3 copies per mL. Thus, it proves a comparable performance compared to the RT-PCR counterpart, which measured N-gene -specific viral loads ranging between a median of about 10^4–10^6 copies per mL for throat swabs, sputum (collected on day 5–6 postonset), and nasal swab samples (collected on day 3 postonset). Another advantage of this electrochemical biosensor is that it allows for detecting early-onset viral load (10^6 copies per mL) of SARS-CoV-2. Thus, it is translatable into the POC testing once the ongoing investigation is completed to simplify the proposed setup and reduce the sample-to-result time.

LAMP operation (**Figure 6**A) relies on autocycling strand displacement employed by a DNA polymerase having high strand displacement activity and a set of target-specific designed inner and outer primers for hybridization and strand displacement.[135] The reaction is conducted at about 60–65 °C and achieved by assessing two noncyclic and cyclic stages. Then, the designed primers are used to detect six distinct regions on the target nucleic acid that can be either DNA or RNA by using a reverse transcriptase enzyme in RT-LAMP assay. This
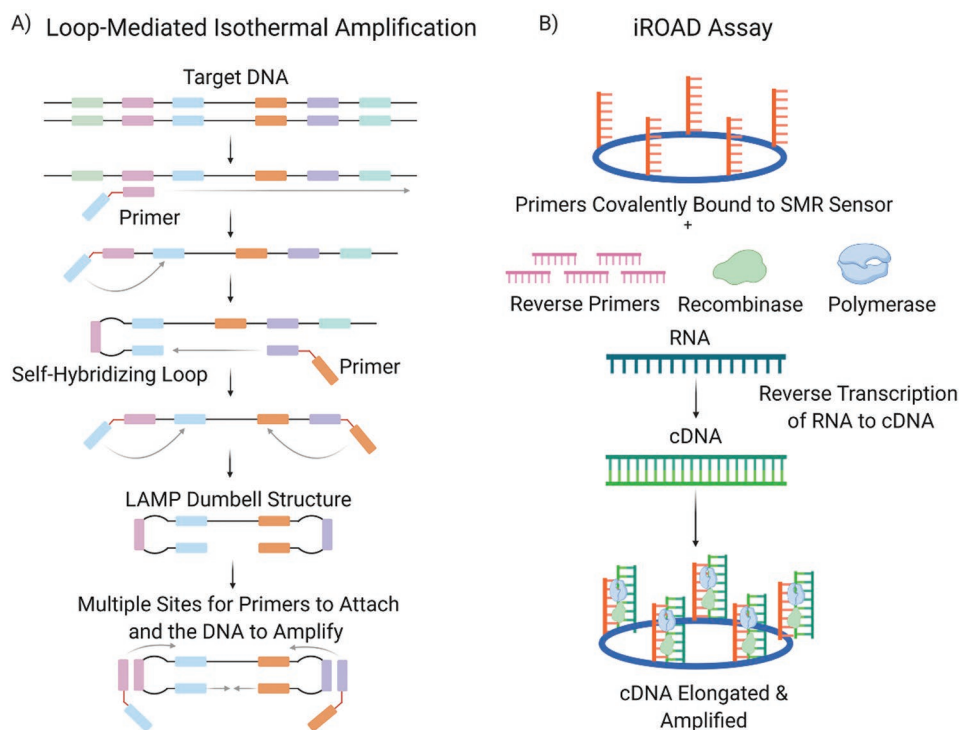
Figure 6. Schematic of isothermal amplification featured in various biosensors. A) Schematic for loop-mediated isothermal amplification (LAMP), in which primers create self-hybridizing loops of target DNA. The self-hybridizing loops assume the LAMP dumbbell structure due to the multiple sites that primers attach to initiate DNA amplification. B) Schematics describing the iROAD assay. Forward primers are immobilized on the surface of the silicon microring resonator (SMR)-based sensor. Next, reverse primers, reverse transcription-recombinase polymerase amplification (RT-RPA) reagent, and patient RNA are added to perform reverse transcription. Double stranded cDNA binds to the forward primers and is amplified and elongated by RPA on the SMR biosensor. All images within this figure are adapted with permission from Biorender.com with a paid academic subscription.

isothermal system offers a rapid, sensitive, accurate, and cost-effective measurement method; therefore, it can be easily adapted for low-cost POC diagnostics, especially in resource-limited settings.[67,135]

In this direction, a one-pot RT-LAMP assay was utilized to detect MERS-CoV virus disease from respiratory samples from infected individuals.[136] The immunoreactions between the biotin/fluorescein/digoxin-labeled duplex amplicons and the streptavidin-conjugated polymerized nanoparticles were detected with a set of two primers, the ORF1ab- and N-genes of MERS-CoV were simultaneously amplified in a single reactor and fluorescently measured. This method is more affordable, more applicable, and offers comparable sensitivity to RT- and qRT-PCR measurements. However, the false-positive readouts due to aerosol contamination at a constant temperature remain critical. Similarly, a multiplexing approach was followed in another one-pot assay to develop an RT-LAMP incorporated with a nanoparticle enhanced LFIA-based biosensor for SARS-CoV-2 detection. In addition, the LFIA results obtained for oro-pharynx swab samples testing indicated no cross-reactivity with non-specific templates, suggesting a foolproof specificity and selectivity for SARS-CoV-2 virus detection.

Another isothermal amplification strategy for the molecular diagnostic is the RPA method performed at relatively low temperatures (≈37 °C to ≈42 °C) and offers fast reaction time with a proper temperature operation.[137,138] Combining the RPA method with an isothermal RNA amplification (iROAD) assay

and an optical detection tool, a silicon microring resonator (SMR)-based biosensing system was developed (Figure 6B).[139] The iROAD-SMR device was tested using nasopharyngeal specimens obtained from patients having different respiratory viruses (IFN-A/B, HCoV-OC43/229E, and RSV-A/B). This study indicates that the iROAD assay could detect as low as 25 copies per reaction, whereas, in RT-PCR, the same signal output can only be obtained if ten times or even more RNA samples exist in the reaction. This high analytical performance obtained for all viruses measured suggests the clinical applicability of this device for detecting different pathogens of interest if newly designed primers accompany it. However, this study needs to be evaluated by integrating sample processing and detection in a miniaturized format to enable POC testing of multiple ana-lytes in various samples such as blood, urine, and sputum.

In another study, the RPA-aided electrochemical biosensor was utilized for the rapid and sensitive detection of SARS-CoV-2.[140] The microelectrode array of an electrochemical sensor allowed for detecting multiple target genes (N-gene and RdRP) without pre-amplification or purification using differen-tial pulse voltammetry. The isothermal RPA reaction involves hybridizing RPA amplicons with thiol-modified primers immobilized on the working electrodes, reducing the current density measured as amplicons accumulated. Although the platform implemented offers a sensitive and on-site measure-ment of the COVID-19, clinical samples from different sources need to be tested. In addition, the multiplexing capability of

the designated biosensor should be evaluated by targeting multiple genes.

As indicated, isothermal amplification methods offer many benefits over PCR, including constant temperature process and shorter assay times (20 min for the iROAD system and 60 min for the one-pot LAMP assay), and higher sensitivities obtained. However, although these methods offer promising tools for determining genes expressed explicitly for a particular viral disease, several problems exist and need to be addressed. For instance, nonspecific amplification may directly affect the assay's sensitivity and specificity due to the lack of a temperature-gating mechanism. In addition, the existence of multiple primers (for example, in the case of LAMP, six primers per target) leads to an increased likelihood of primer dimerization and is problematic. Therefore, avoiding primer-dimer formation and amplification while performing the assay and classifying reactions as either specific or non-specific amplification are crucial points; hence, assay optimization needs to be identified to get optimum performance and deployment in on-site diagnostics.[141,142] Also, most isothermal assays are laborious and expensive, still requiring an RNA extraction step using costly kits. In the case of high demand, such as in pandemic situations, the shortage of these kits can be precarious.[143] Furthermore, developing advanced tools for isothermal amplification that would enable affordable, quick, extraction-free, and efficient detection of various pathogens-associated genetic biomarkers in a multiplexed device simultaneously is of great interest.

3.2.2. Nucleic-Acid Probe-Based Biosensing

Single-stranded DNAs (ssDNAs), RNAs, or peptide nucleic acids (PNAs) act as molecular recognition elements via hybridization. In the case of viral pathogens, RNA is first extracted from the virus. This isolate is exposed to biosensors with oligonucleotide probes immobilized on the surface, enabling a measurable response for viral detection (**Figure 7**). These probes are short nucleic acid sequences that can hybridize to target analyte single-stranded DNA or RNA based on NA complementarity and be labeled (radioactively, fluorescently, etc.) using synthetic target molecules. Herein, similar to immunoassays, both sandwich and competitive assays could be realized.[144]

Using multiple oligonucleotide probes modified to an SPR chip, simultaneous detection of several respiratory viruses, including Influenza A and B and SARS, was achieved.[145] After carboxyl group formation and surface activation of the self-assembled monolayers (SAM), specifically designed respiratory virus probes were printed onto the functionalized gold surface. Following RNA extraction, the amplification of the target RNAs was achieved by multiplexed RT-PCR using biotin-labeled primers. The SPR signal intensities that were shifted due to the hybridization reaction between the PCR-amplified viral genome and oligonucleotide probe on the gold surface were tested in the presence of streptavidin. Combining the Au gene chip with RT-PCR, the biosensor claims high specificity and high-throughput detection within 30 min. However, due to its bulky
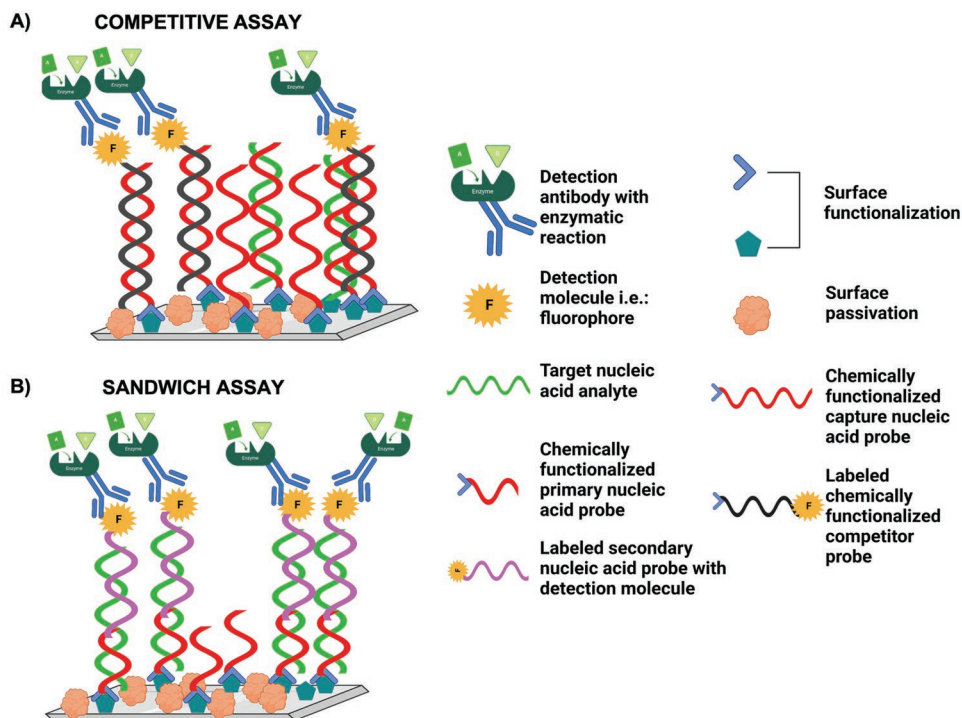
Figure 7. Oligonucleotide probes are immobilized on the biosensor surface for hybridization of target RNA/DNA. A) Competitive oligonucleotide hybridization: Extracted pathogen single-stranded RNA hybridizes to the complementary oligonucleotide. Additionally, a labeled competitor probe has complementarity to the surface-functionalized probe and acts for the same hybridization sites and elicits a biosensor response (for example, electrical). Target analyte concentration is inversely proportional to competitor signal. B) Sandwich assay-based oligonucleotide hybridization: Short primary nucleic acid probe, complementary to target RNA/DNA, is functionalized to surface. Target pathogenic RNA/DNA is introduced first, which followed by a labeled secondary probe (complementary to target RNA) hybridizing to the distal end of target RNA for production of measurable response. All images within this figure are adapted with permission from Biorender.com with a paid academic subscription.

2201085 (15 of 30)

**ADVANCED
SCIENCE NEWS**

www.advancedsciencenews.com

**ADVANCED
MATERIALS**

www.advmat.de

instrumentation, further miniaturization is required prior to its use at the point of care as a complementary diagnostic method.

Another genosensor incorporating thiolated oligonucleotide probes onto gold nanostructured screen-printed carbon electrodes was employed to detect the SARS-CoV virus via hybridization.[146] Streptavidin-labeled alkaline phosphatase (AP) was used as an enzymatic label that catalyzed the dephosphorylation of the 3-indoxyl phosphate substrate, resulting in silver ions reduction in the solution and screened by voltammetry measurements. Even single base-mismatched complementary strands could be efficiently detected with the developed genosensor, suggesting high selectivity and pM sensitivity. This high analytical performance offers promise when considering SARS-CoV-2 variants, where the different variants consist of specific substitutions of bases within the spike protein section of the viral genome.[147]

PNAs were seen for the application of detecting MERS-CoV, mycobacterium tuberculosis, and human papillomavirus (HPV) in tandem in a recent study that developed a multiplexed sensor that was integrated with a pyrrolidinyl PNA– nanoparticles. Upon hybridization, the paper-based colorimetric assay allowed for viral DNA detection. The multiplexed capability, ease of use, and ability to detection DNA associated with both viral and bacterial infections, and simplicity of a paper-based colorimetric assay show great promise as a low-cost and disposable alternative for rapid triaging at the POC. However, given that selectivity was reduced with one- and two-base mismatches, further optimization is required before adoption in a clinical setting.[131]

A unique application incorporating PNAs has recently utilized the hybridization capabilities of the synthesized PNAs as a blocking mechanism to measure human SARS-CoV-2 specific gene sequences more sensitively, as compared to bat and other SARS-related coronaviruses through the conserved sequences of ORF3ab E-and N-genes.[148] This blocking technique aimed to discriminate between SARS-CoV-2 and other SARS related-CoVs in human samples without compromising sensitivity. The sensitivities were significantly increased in both detections when the designed PNAs probe was combined with an RT-qPCR workflow. PNAs are considered to be "synthetic DNAs" where the typical phosphodiester backbone seen in DNA is replaced with a 2-aminpethylglycine chain. However, PNAs cannot serve as primers for polymerization and eventual amplification of target sequences but are still able to bind nucleobases complementary in target DNA or RNA samples. Thus, PNAs are great tools for exploiting the blocking effect of amplification. In this study, the designed PNAs effectively block RT-qPCR amplification of SARS-CoV for N-gene, where 100-fold more RNA copies per reaction are needed to detect SARS-CoV N compared to SARS-CoV-2 N transcript. Although these results were not directly involved as a biosensor, the promising results can be translated to a biosensor modality for large-scale testing of SARS-CoV-2 and other novel viruses and discerning true-positive versus false-positive cases from other SARS-related coronaviruses.

Using an automated microfluidic sample preparation multiplier (SPM) along with optofluidic ARROW system, amplification-free detection of the Ebola viruses in clinical samples was achieved.[149] The SPM microfluidic chip consists of incubation reservoirs, liquid-core and solid-core waveguides, and input and output channels with the capability of performing six assays in parallel. Pressure valves facilitate the automated on-chip fluid transfer. Magnetic beads were functionalized with NA capture probes and added to the incubation reservoirs. Ebola virus RNAs extracted from clinical samples were then hybridized to the complementary capture probes. Zaire Ebola virus RNA as the positive control and Sudan Ebola virus RNA as the negative control were used. Captured targets are released by heat denaturation and concentrated three-fold. ARROW fluorescence detection utilizes a lens-adapted optical fiber and spectrometer to detect the target RNA. The novel SPM improves the previous optofluidic design[150] by enabling metered air bubbles. Thus, it enhances the target capture without a need for additional devices or increasing fabrication complexity. Additionally, it requires only minimal user interaction owing to the automated process for sample preparation. This amplification-free optofluidic device offers a unique alternative to PCR for viral detection with its low LOD (2.1×10^{-3} PFU mL^{-1}) and sample-to-result time of less than 2 h. Such a high sensitivity allows even to diagnose pre-symptomatic infections before the onset of severe symptoms. All these features make this system an ideal candidate for clinical and POC testing, however, more attention should be paid to miniaturization and multiplexing for an increased throughput.

In another optofluidic configuration, silicon nitride waveguides were realized in nanoslots, forming a femtoliter fluidic channels, to detect the fluorescently tagged product of reverse transcription of the N gene virions of the SARS-CoV-2 virus in real time.[151] Using transverse electric polarized light, the optical field overlapped within the fluidic slot channel confines the light at a rate of 50.5%, greatly increasing the light–matter interaction; hence the sensitivity of the biosensor developed. The fluorescence emission of the cDNA is carried to a spectrometer via a small fiber. This platform could discriminate between the cDNA from SARS-CoV-2 and that from stereotype 1 Dengue viral RNA from only a 40 fL sample volume. While reverse transcription is required to translate target RNA into fluorescently labeled cDNA, the amplification-free nature of this approach decreases the running costs and increases its accessibility in clinical settings. Another benefit of this platform is that the assay functions at a wide range of pHs and temperatures with minimal sample preparation. Nonetheless, the operation of this platform necessitates a large and expensive optical equipment, including the laser and the waveguide, which may be limiting its POC utility.[151]

3.2.3. CRISPR-Cas-Powered Biosensors

Previously, CRISPR, and its generated customizable RNA-guided nucleases, such as Cas9, have been used to quickly, simply, and efficiently transform endogenous genes in a wide variety of cell types and in organisms that have been challenging to manipulate genetically using conventional approaches.[152] In addition, using their ability to recognize and cleave specific DNA and RNA sequences, several applications, including gene editing,[153,154] genome imaging,[155] have been proposed. Lately, many efforts have been directed towards understanding their potential in nucleic acid-based diagnostics.[148,156–158]

A wide variety of CRISPR-Cas enzymes is presently available for programmable recognition of DNA and RNA sequences classified into two main groups based on the organization of their loci and signature proteins.[159] While the Class I CRISPR-Cas systems employ multiple subunit effector complexes, Class II (for example, Cas9, subtypes Cas12, Cas13) group uses single RNA-guided Cas proteins to recognize and cleave target nucleic acid sequences and are viable tools when adapted for pathogen detection.

Among DNA targeting Cas proteins, Cas9 enzyme guided by single-guide RNA (sgRNA) can specifically bind to target double-stranded DNA (dsDNA), cleaves it due to the nuclease activity, and eventually result in a DNA double-strand breakage.[160,161] The first proof-of-concept study based on CRISPR-Cas9 has been utilized by merging in silicon technology with the NASBA method for primer generation optimal and toehold switches for Zika virus (ZIKV) detection.[161] A microfluidic paper-based analytical device, including freeze-dried reagents for isothermal RNA amplification, in combination with a portable readout device, was used to screen the colorimetric changes upon viral RNA detection. The proposed sensing methodology holds an excellent promise for multiplexed adaptation to strain-specific detection of the various nucleic acids would be a viable tool to monitor several infectious diseases by specifically designing primers, especially in low-resource settings.

An alternative class of Cas protein, Cas12, is a proficient enzyme that possesses the *cis–trans* cleavage activity of ssDNA creates staggered cuts in dsDNA and is being used for pathogen detection (**Figure 8**A).[162] For example, a DNA endonuclease targeted CRISPR trans reporter method was developed based on the activation of Cas12a ssDNase. The signal enhancement was achieved by combining it with RPA for nucleic acid amplification.[163] Targeted DNAs of papillomaviruses, specifically HPV16 and HPV18, were detected testing human serum samples by utilizing LFIA. The results obtained from the CRISPR-Cas12a technique presented a good correlation with the PCR assay. Also, its easy integration to a mobile phone device for optical readout, suggesting its suitability for on-site use. Similarly, another DNA probe method based on a CRISPR-Cas12

target cleavage enhanced by an RT-LAMP assay, so-called DNA endonuclease-targeted CRISPR trans reporter (DETECTR), was proposed for on-site diagnosis of the COVID-19 disease.[127] The RNA samples were extracted from the nasopharyngeal or oro-pharyngeal swab, amplified, and tested through Cas12 detection of predefined coronavirus sequences. After assessing synthetic primers, which are designed to target the E- and N-gene regions of the SARS-CoV-2 virus, the cleavage of a reporter molecule confirmed that the targeted virus is present in each sample. The reaction results were visualized using both fluorescence readers and lateral flow strips designed to capture labeled nucleic acids, showed no cross-reactivity across other coronaviruses (SARS-COV, bat SARS-like coronavirus) tested. Considering the encouraging predicting power (100% negative, 95% positive predictive agreement with the real-time RT-PCR), high-speed development, and validation process (≈2 weeks), this assay offers versatility to be adapted to identify viral pathogens, especially after multiplexing has been applied.

While some Cas enzymes target DNA (Cas9, Cas12), single RNA-guided effector proteins, such as Cas13 (Figure 8B), can be engineered to pursue a specific recognition and cleavage activity towards the complementary CRISPR RNA (crRNA).[164,165] Due to the trans and collateral cleavage activity of nearby RNA, Cas13 RNases have been extensively used to detect viral RNA transcripts in patient samples. For example, by incorporating CRISPR-Cas13 RNA detection assay to a previously developed microchamber-array technology, the "CRISPR-based amplification-free digital RNA detection (SATORI)" platform was established to perform N-gene targeted SARS-CoV-2 detection.[156] The SATORI system allows for amplification-free (fM-range), rapid (within 5 min), and simultaneous detection of multiple targets of different sites in the SARS-CoV-2 N-gene using three crRNAs complementary to different regions of the target RNA. This concurrent use of multiple crRNAs is important in this study because the Cas13-gRNAs used may target different regions of target RNA and thus, expose the potential for false positives. Besides, combining these three crRNAs for the same target results in an enhanced sensitivity. The screening can be performed by a compact fluorescent microscope, to
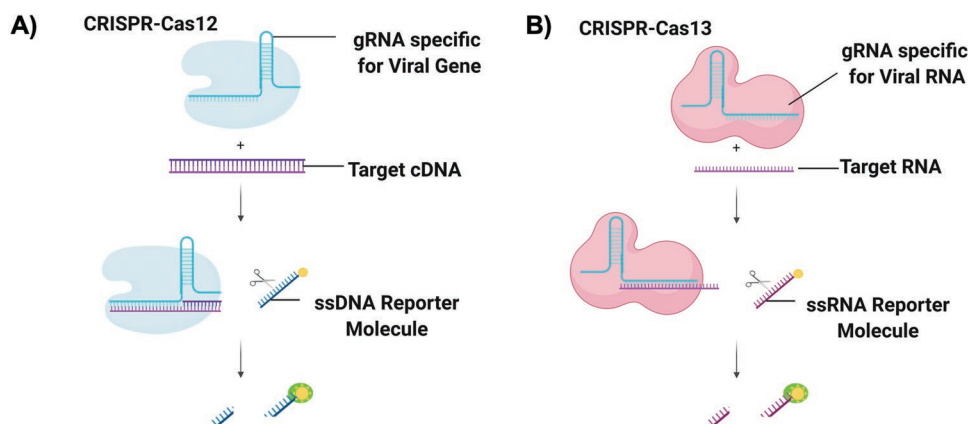
Figure 8. CRISPR-based assays for detecting viral RNAs. A) Cas12 enzyme recognizes complementary DNA (cDNA) produced by the reverse transcription of the viral RNA. The binding of cDNA activates non-specific nuclease activity on ssDNA. B) Recognition of viral RNA by Cas13 enzyme activates non-specific ribonuclease activity on ssRNA. Both activities are utilized to cleave the ssDNA/ssRNA reporter molecules, respectively, to amplify the fluorescence upon cleavage. All images within this figure are adapted with permission from Biorender.com with a paid academic subscription.

**ADVANCED
SCIENCE NEWS**

www.advancedsciencenews.com

**ADVANCED
MATERIALS**

www.advmat.de

which many clinical labs already have access, supporting the clinical applicability of this platform. In addition, this platform could be directly applied to clinical samples without any RNA purification thanks to the robustness of SATORI against contaminants including nontarget RNAs, virus transport media, saliva, and different swabs. However, since there is a need for a fluorescence microscope and image processing software for accurate analysis, SATORI does not currently appear to be amenable for resource-limited (such as at-home) settings.

Similarly, another amplification-free proof-of-concept study based on CRISPR-Cas13a detection was presented to detect the SARS-CoV-2 RNA from extracted patient nasal swab samples by combining multiple crRNAs targeting different regions of the viral RNA genome.[132] The fluorescent signals obtained are quantitatively measured using an integrated portable mobile phone camera-based device. Uniquely, this study employed multiple crRNAs to increase Cas13 activity (i.e., sensitivity), analyzed the change in fluorescence over time with Cas13 activation, which allowed the detection of ≈100 copies μL^{-1} from SARS-CoV-2 patient samples within 30 minutes. Although the results of this study are promising due to allowing sensitive and rapid, and low-cost detection of SARS-CoV-2 RNA measurements without any RNA amplification, POC adaptation can be achieved if the lab-based RNA extraction step is replaced with an extraction-free protocol.

Although encouraging achievements have been obtained by employing CRISPR-Cas-powered detection strategies, there are still many challenges to overcome before this method can replace the well-established nucleic acid detection techniques, for instance, RT-qPCR.[166] Most of the developed assays still comprise a preamplification step to achieve lower LODs which disrupts direct analysis of a given sample, increases the sample-to-answer time, and the misinterpretation risk of the results due to amplification errors.[156] In addition to amplification-free protocols, replacing lab-scale RNA extraction steps with extraction-free procedures will decrease the assay's complexity for the end-user and turnaround time and bring us to the CRISPR-powered POC diagnostic platforms intended one step closer (**Table 2**).

3.3. Biosensors for the Detection of the Host Immune Response

Upon virus entry, the host's immune system produces various inflammatory biomarkers, like antibodies, cytokines, and chemokines, to combat the viral infection.[78,169] While antibody detection is achieved to determine the presence of viral infections or the immunity against a virus, pro-inflammatory cytokines and chemokines are mainly employed to monitor the antiviral immune response and predict the expressed disease pattern. Understanding diverse disease pathology leads primarily to developing treatment and prevention strategies.[78,79]

3.3.1. Antibody (Immunoglobulin) Detection

Antibody testing is not only critical for evaluating acquired immunity features but is also essential in vaccine development.[170] The production of antibodies results from an immune defense response against the prior expression of the external antigen by the disease-related genome. Hence, antibodies are a crucial indicator of inflammatory diseases due to providing several possibilities that ease disease management, including the diagnosis, progression screening, understanding the pathology of conditions, and accordingly developing subsequent therapy.[171] Viral pathogen-associated antibody detection can be performed by testing body fluids, including blood and swab samples. The presence of antibodies targeting the receptor-binding domains (RBD) of the structural virus constituents can be determined qualitatively and quantitatively.[34]

The detection of host-immune response-associated antibodies is achieved by utilizing pathogens and pathogen-specific proteins (N, S, and E proteins) as biorecognition molecules (**Figure 9**). In detail, upon viral infection, the immune system produces IgMs for a prior immune defense, and its level is commonly quantified for rapid identification of the disease exposure. Following that, an adaptive and high-affinity IgG response is created to neutralize viral pathogens, which are screened to assess previous exposures to a particular infection, acquired long-term immunity, and immunological memory features.[172]

In current clinical practice, the quantitative detection of antibodies is mainly achieved by conventional ELISA systems, microparticle enzyme immunoassay (MEIA), and western blot. However, several factors, including the need for expensive and bulky instruments, multistep and time-consuming operation processes, and various reagents, of these assays limit their applicability in POC testing. For the qualitative or semiquantitative on-site testing of antibodies against viral infections, LFIAs, also known as at-home pregnancy/ovulation tests, have been extensively employed. However, immunoassay-based techniques such as LFIAs lack sensitivity and reliability due to high cross-reactivity between similar antibodies.[173,174]

Unlike traditional LFIA assays that use colloidal AuNPs or other fluorescent dyes as optical labels, LFIAs, along with lanthanide-doped polystyrene NPs (LNPs), demonstrated an enhanced measurement performance (such as high stability, quantum yield, and sensitivity) compared to its conventional peers such as gold.[175] In this setup, N proteins of SARS-CoV-2 were first dispensed onto a nitrocellulose membrane to capture specific IgGs. Then, the self-assembled LNPs that served as fluorescent reporters were coupled with anti-human IgG antibody and rabbit IgG. The functionalized LNPs mixtures were separately dispensed onto the lateral flow test strip and incubated for 10 min. Excitation of the LNPs at 365 nm wavelength resulted in a fluorescence shift at 615 nm on the test line upon antibody binding. The intensities of the test and the control line were recorded with an embedded portable fluorescence reader. The ratio of both lines was calculated to determine the anti-SARS-CoV-2 IgG concentration in the human serum samples analyzed. Furthermore, SARS-CoV-2-related IgG antibody detection and disease progression monitoring were performed simultaneously using this platform; hence it can be adapted to other viruses' detection, especially in low resource settings.

There is no doubt that both IgM and IgG antibody assays alone give essential information about specific disease pathology; however, when the corresponding disease-related antigens are combined in a single platform, better utility and

Table 2. Biosensors for indirect pathogen detection (IA: isothermal amplification, NPs: nanoparticles, HAU: hemagglutinating unit, PDMS: polydimethylsiloxane, ORF1ab: opening reading frame 1a/b, HCoV: human coronavirus, RSV: respiratory syncytial virus, RPA: recombinase polymerase amplification, ZIKV: Zika virus, DENV: flavivirus dengue, PIV: parainfluenza virus, ADV: adenovirus, SELEX: systematic evolution of ligands by exponential enrichment, RCA: rolling circle amplification, MDA: a12-mercaptododecanoic acid, HuNoV: human norovirus, cDNA: complementary DNA, PFU: plaque-forming unit, Si: silicon, SiO_2: silicon oxide, Si_3N_4: silicon nitride, PEDOT:PSS: poly(3,4-ethylene dioxythiophene) polystyrene sulfonate, HA: hemagglutinin, ITO: indium tin oxide, SPCEs: screen-printed carbon electrodes).

Detection method	Disease	Transducer	Sensor/Electrode material	Surface modification	Receptor	Target	Sensitivity	Linear range	Turn-around time	Refs
NA-probe hybridization	SARS-CoV-2	Electrochemical	Carbon	SiNPs	RCA product	N and S genes	1 copy μL^{-1}	$1-1 \times 10^9$ copies μL^{-1}	<2 h	[130]
Colorimetric LAMP assay	Influenza A MRSA	Optical	PDMS	Affinity molecule conjugated magnetic beads	H1N1 specific aptamer Vancomycin conjugated magnetic beads	H1N1 MR bacteria	3.2×10^{-3} HAU per reaction	$3.2 \times 10^{-1} - 3.2 \times 10^{-5}$ HAU per reaction	40 min	[67]
Colorimetric LAMP assay	SARS-CoV-2	Optical	Nitrocellulose membrane	Polymerase NPs	Anti-Dig Ab Anti-FITC Ab Biotin-BSA	ORF1ab and N genes	12 copies per reaction	$1.2 \times 10^4 - 1.2 \times 10^1$ copies μL^{-1}	1 h	[136]
Long oligonucleotide arch-shaped hybridization	Influenza A and B	Optical	Si	cDNA synthesis and amplification	Primers of IFN, HCoV, and RSV	Viral RNA of IFN, HCoV, and RSV	25 copies per reaction	$25 - 10^9$ copies per reaction	<20 min	[139]
Surface hybridization with a complementary strand	SARS-CoV-2	Electrochemical	Au/PDMS	Thiol-modified nucleotide hybridization	Thiol-modified primer	RdRP and N genes	0.972 fg μL^{-1} 3.925 fg μL^{-1}	$10^3 - 10^9$ copies μL^{-1}	<20 min	[140]
LAMP-RT & CRISPR-Cas12	SARS-CoV-2	Optical	Lateral flow strip	FAM-biotinylated reporter molecule	Cas12 with gRNAs	E and N genes	10 copies μL^{-1}	0-2500 copies μL^{-1}	<40 min	[127]
CRISPR-Cas13a	ZIKV DENV	Optical	Reaction tube	N/A	Cas13a with crRNAs	ssRNA-ZIKV ssRNA-DENV	2×10^{-18} m	$10^1 - 10^4 \times 10^{-18}$ m	5 min	[165]
Novo-designed prokaryotic riboregulators (Toehold switches) for ZIKV CRISPR-Cas9	Zika virus	Optical	Paper-based disc	Primers, toe hold switches, Cas9	dsDNA with trigger H and strain-specific PAM Cas9	RNA genome of Zika virus	2.8 fM	$0 - 3$ μM	3 h	[161]
CRISPR-Cas	SARS-CoV-2	Optical	Chrome on a glass substrate	Cas13a-crRNA-tgRNA complex	Cas13a with crRNA	N gene	5.7×10^{-15} M	$10^{-3} - 10^4 - 10\text{-}12$pM	<5 min	[156]
CRISPR-Cas	SARS-CoV-2	Optical	PDMS	Cas13a-crRNA RNP	Cas13a with multiple crRNAs	N gene	≈ 100 copies μL^{-1}	$1.8 \times 10^2 - 1.35 \times 10^3$ copies mL^{-1}	<30 min	[132]
NA-probe hybridization	Influenza A Influenza B PIV1 RSV ADV SARS H1N1	Optical	Au	12-mercapto-dodeca-noic acid (MDA) via amine chemistry	Amine labeled virus-specific oligo-nucleotide probe	PCR products from virus-specific RNA	5×10^{-9} m $1 \times 10\text{-}9$ M $1-3.5 \times 10^{-9}$ M 3×10^{-9} M 0.5×10^{-9} M 2×10^{-9} M 3×10^{-9} M	N/A	Real-time	[145]
Enzyme-linked aptamer hybridization	HuNoV; Snow Mountain Virus (SMV)	Electrochemical	Polystyrene well plate	Viral like particles	Biotinylated aptamer	SMV and HuNoV protein	10 RNA copies of lettuce per sample	10 nM – 2 mM	3 h	[167]

ADVANCED
SCIENCE NEWS
www.advancedsciencenews.com

ADVANCED
MATERIALS
www.advmat.de

Table 2. Continued.

| Detection method	Disease	Transducer	Sensor/Electrode material	Surface modification	Receptor	Target	Sensitivity	Linear range	Turn-around time	Refs
Oligonucleotide probe hybridization	Ebola	Optical	Glass substrate with PDMS microfluidics	Streptavidin	5' Amino Modifier C6 oligo nucleotide probe	Zaire Ebola virus RNA	0.021 PFU mL^{-1}	10–10^3 PFU mL^{-1}	40 min	[149]
Fluorescent cDNA	SARS-CoV-2	Optical	Si/SiO$_2$/Si$_3$N$_4$	N/A	Fluorescent tagged cDNA	N gene	10^9 copies mL^{-1}	1–10 × 10^{-6} M	Real-time	[151]
NA-probe hybridization	Influenza A	Electrochemical	PEDOT:PSS	IAV Aptamer	Poly(T)-Poly(C) linker and Int Spacer 9	Influenza A virus	N/A	200 × 10^{-6} M	35 min	[168]
NA-probe hybridization	H1N1	Electrochemical	Au	Thiolated aptamer probe with spacer, HS-A20S	H1N1 specific aptamer	Inactivated Influenza viral particles	0.9 pg µL^{-1}	5.5 – 45 ng mL^{-1}	Real-time	[118]
NA-probe hybridization	Influenza A	Electrochemical	ITO/glass	Charge interaction; ITO-polyethenimine (PEI)-V46	V46 aptamer	IVA mini- HA protein; whole H1N1 virus	3.7 PFU mL^{-1}	10–10^3 PFU mL^{-1}	2 h	[119]
NA-probe hybridization	SARS	Electrochemical	SPCEs	AuNPs	3' biotinylated probe; 3' thiolated probe	SARS N protein DNA sequence	2.5 × 10^{-12} M	2.5–50 × 10^{-12} M	20 min	[146]
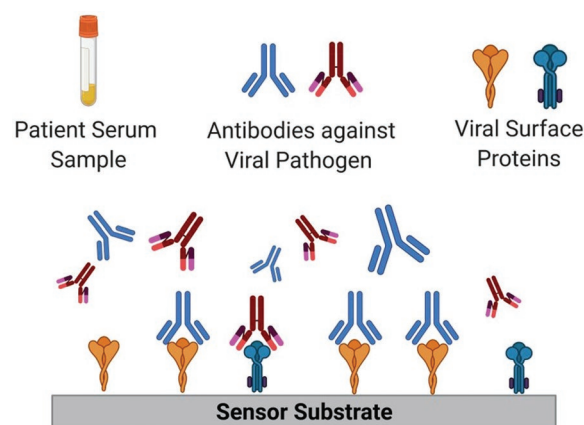
Figure 9. Biosensors for host immune response detection. Surface of the sensing area is functionalized with viral antigens to detect the presence of neutralizing antibodies produced as a response to a viral infection. Binding of the target antibody to its antigen leads to a measurable signal. All images within this figure are adapted with permission from Biorender. com with a paid academic subscription.

sensitivity could be obtained. A combinatory kit was developed using an LFIA to qualitatively and rapidly detect IgG–IgM antibodies against SARS-CoV-2.[25] The LFIA strips were separately modified spraying SARS-CoV-2 S protein fused AuNPs, which allowed the detection of IgG and IgM antibodies in whole blood, serum, and plasma samples of patients, presenting more informative results than the IgG and IgM tests alone. Therefore, such LFIA platforms should be improved to conduct quantitative analyses to evaluate epidemiological factors such as the extent of viral infection age-ranked seroprevalence and to study impermanent immunity features.[27,176]

Compared to LFIA tests, electrochemical biosensors offer more accurate, rapid, and highly sensitive tools for on-site quantification of immune response antibodies against viruses. For instance, an impedimetric sensor for detecting circulating ZIKV antibodies from saliva and undiluted serum samples of human subjects was presented.[174] Herein, screen-printed carbon electrodes enhanced with carboxylated carbon nanotubes were coated with recombinant structural protein domains, domain III of the E protein, and a fragment of a nonstructural protein were employed as bioreceptors to detect ZIKV-specific antibodies. To achieve this, the biosensors need to be first incubated with the diluted serum sample before being exposed to secondary antibodies (anti-IgM-Ab2 or anti-IgG-Ab2), followed by the impedance measurement. Although the satisfactory performance was achieved for the differentiative detection of the ZIKV-specific immune antibodies, the multi-stage assay format needs to be simplified to use this biosensor in the POC settings.

In another study, antihepatitis B IgG antibodies were gauged via sandwich immunoassay on an electrochemical biosensor where magnetic beads were employed for immunoreactions and AuNPs for electrocatalytic labeling.[177] A rapid and straightforward IgG measurement was achieved by chronoamperometric detection of the electroreduction of hydrogen ions in an acidic medium. Although the proposed method represents a low-cost and more sensitive alternative to traditional LFIA testing, it is still not suitable for POC testing unless complicated fabrication

steps are simplified, and laborious instruments are miniaturized for on-site testing.

Detecting viral infections by identifying host-immune-associated antibodies could be enlightening and a robust strategy than the counterpart approaches. So far, there are many well-established (and even commercialized) LFIA-based and other biosensing platforms. By putting more effort into enhancing the performance of these devices (i.e., increasing the sensitivity and eliminating cross-reactivity) and miniaturization, they can be used as quantitative analysis tools in limited-resource settings, especially during pandemics where the rapid diagnosis is essential to manage a potential outbreak.

3.3.2. Detection of Proinflammatory Biomarkers

The innate immune system uses a variety of pattern recognition receptors (PRRs), including C-reactive protein (CRP) and serum amyloid protein (SAP), that are synthesized as an acute phase response to a specific infection.[178,179] The primary roles of PRRs include opsonization (via CRP and SAP), activation of complement and coagulation cascades, phagocytosis, activation of pro-inflammatory signaling pathways, and induction of apoptosis.[180]

In a typical viral infection scenario, the cellular response is either mediated by transcriptional cytokine induction, including interferon (IFN) and upregulation of IFN-stimulated genes (ISGs), or leukocytes and their subgroups mainly created by chemokine discharge.[179,181] For instance, cytokines are regulators of the host response to infection, which can modulate the inflammatory response, clearance pathogens, and ensure the repair of infected tissues. While the proinflammatory cytokines make the disease worse, the anti-inflammatory types reduce inflammation and stimulate healing.[182,183]

Detection of proinflammatory biomarkers is important in characterizing varying antiviral defense mechanisms and their contributed components at a molecular level. For instance, the disease severity of COVID-19 patients was found correlated to elevated serum levels of the IL-6, IL-10, IL-2, interferon-γ(IFN-γ), tumor necrosis factor-alpha (TNF-α), and CRPs.[184] Indeed, some of these pro-inflammatory biomarkers, precisely IL-6 and CRP, were found to have a predictive value for lung inflammation and used to determine patients requiring ventilation.[185] On the other hand, the elevated production of the pro-inflammatory biomarkers caused a "cytokine storm" yields subsequent tissue damage resulting in multi-organ failure, hence the mortality.[186,187] Although targeting pro-inflammatory biomarkers for viral infectious disease management could improve survival rates, these biomarkers are present at low concentrations in different sample types (including serum, sweat, tears, and urine) tested. So far, several analytical procedures, including immunoassays (such as ELISA), molecular biology techniques, and flow cytometry, have been applied for evaluating cytokine levels in body fluids, tissues, and cells. However, most of these methods, particularly ELISA, suffer due to their insufficient sensitivity and multistep/time-consuming procedures, inhibiting its use in on-site monitoring. Hence, biosensors that can sensitively, accurately, and rapidly detect proinflammatory biomarkers on site are of great interest.[129,188]

Though designing and prototyping biosensors for detecting pro-inflammatory biomarkers are challenging due to the following factors: i) cytokines are found at pg mL^{-1} levels in a blood-based specimen, ii) to obtain bedside information, the tests should be realized by directly utilizing untreated samples (like urine, whole blood, saliva, sweat), iii) as the oversaturation of hospitals in pandemic situations does not allow for long-term (and preferably continuous) screening of all severely ill patients, decentralized care should be assimilated by designing portable biosensing devices for at-home or wearable testing.

For instance, LFIA tests combined with surface enhanced Raman spectroscopy (SERS) were developed for IL-6 detection in untreated whole blood samples.[189] The nitrocellulose membrane was functionalized with SERS tags (Raman signaling molecule-modified silica oxide–gold core–shell NPs) and anti-IL-6 antibodies. Raman intensities changed with the detected IL-6 concentrations could be qualitatively seen by the naked eye using the test strips. On the other hand, a Raman spectrometer should be employed to obtain quantitative information. Compared to the conventional LFAs, the SERS-based LFIA proved better sensitivity, shorter turnaround times, and negligible interferences whether tested in serum or whole blood. However, this platform needs to be miniaturized to increase its accessibility and applicability for POC detection.

A multiarray detection platform named a pencil-like immunosensor was established for the on-site detection of 3 inflammatory biomarkers: IL-6, procalcitonin (PCT), and CRP.[190] The suit-case-like portable immunosensor device contains an optical-fiber-based biosensor, a pencil cap-like multiple reagent wells, a photon-counting head powered by a battery that directly converts immune recognition into a luminescent signal, and a touch-screen laptop for data acquisition, analysis, and reporting. Each optical fiber was immobilized with antibodies to form a biorecognition layer and simultaneously used as a signal transducer. While detection, the pencil-like probe was introduced into different wells (with the pre-prepared reagent and sample solutions, detection antibody, signaling complex, chemiluminescence substrate, and washing buffer) on the reagent strip separately in "plug-into/out" format to proceed with multiple detection steps (including sandwich immunoreaction, signal amplification, and chemiluminescence reaction) (**Figure 10**). Although this device is portable, user-friendly, and enables multiplexed detection of biomarkers consecutively, it needs further evaluation to achieve higher sensitivity and simultaneous detection of various analytes.

Enabling fast, real-time and label-free detection of biomarkers, localized surface plasmon resonance (LSPR) systems have drawn much attention and can replace existing fluorescence-based methods.[191] In addition, several features, including their rapid sensor response, inhibited reaction to external interferences, high stability in complex matrices, and non-invasiveness while sample detection make them favorable for real-time testing. Following that, a massively parallelized multiarrayed LSPR chip was developed using microfluidics for the high-throughput detection of multiple cytokine biomarkers in serum.[192] The microarrays were modified by gold nanorods conjugated with antibodies unique for each cytokine protein (IL-2, IL-4, IL-6, IL-10, TNF-R, and IFN-γ). Following the sample introduction, the scattered light intensity was measured
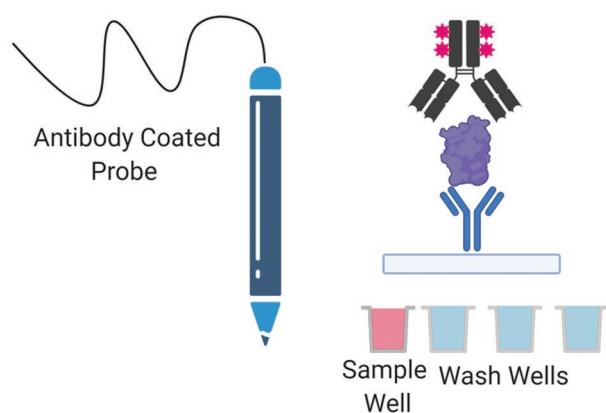
Figure 10. Pencil-like immunosensor. It utilizes an antibody-coated probe to subsequently detect multiple inflammatory biomarkers using a sandwich assay. All images within this figure are adapted with permission from Biorender.com with a paid academic subscription.

using simultaneous replicated measurements, and quantitative information regarding target analytes was collected. The most striking feature of this particular device is its multiplexed and massively parallelized format and low (1 µL) sample requirement needed for detection, which make it highly capable of commercialization for the parallelized detection of various inflammatory serum biomarkers. However, the manual sample preparation setup and bulky optical detection apparatus should be improved and miniaturized to achieve such detection on site.

Besides optical detection methods, electrochemical detection of inflammatory biomarkers is also extensively studied for cytokine detection. For example, graphene oxide (GO)-modified sandwich immunoassay was developed for simultaneous detection of cytokines, IL-6, IL-1β, and TNF-α in whole mouse serum.[193] Each detection antibody was covalently bound to GO-based redox probes to produce signal reporters. On the other hand, the capturing antibodies were covalently attached to the glassy carbon electrode to realize an electrochemical sandwich immunoassay. The signals (obtained by amperometry and square wave voltammetry), exerted by signal reporters and altering when a specific biorecognition reaction occurred between mouse serum spiked multiple cytokines and detection antibodies, were recorded. Although satisfying sensitivity, selectivity, and long-term stability of the functionalized immunosensor were obtained to measure multiple cytokines in spiked serum samples simultaneously, patient sample testing should be carried out to demonstrate its POC testing capability.

Identifying and long-term monitoring the virus-specific inflammatory markers lead to a better understanding of disease-related features than solely detecting a viral pathogen; hence, the existence of inflammatory biomarkers should be carefully identified.[194] Unfortunately, only a few biosensing devices were established to understand the aftermath of the infection by assessing the relationship between the host and particular viral infection-related (pro)inflammatory biomarkers. However, these sensors are neither in clinical settings nor informative enough. Therefore, a similar effort in developing diagnostic tools should be inserted to evolve more informative combinatory devices that allow diagnosis and immune response (**Table 3**).

Table 3. Biosensors for the detection of immune response-related biomarkers upon viral infection (Au: gold, ZIKV: Zika virus, DENV: flavivirus dengue, NC: nitrocellulose, SPCEs: screen-printed carbon electrodes, LNPs: lanthanide-doped polystyrene nanoparticles, mIU: milli-international unit, PBA: 1-Pyrenebutyric acid, IL-6: interleukin-6, PCT: procalcitonin, CRP: C-reactive protein, NRs: nanorods, GO: graphene oxide, Abs: antibodies, M-HIgG: mouse anti-human IgG antibody, RIgG: rabbit IgG, 3-ADMS: 3-aminopropyl diethoxymethylsilane, EDC:1-ethyl-3-(3-dimethylaminopropyl) carbodiimide hydrochloride, NHS: N-hydroxy-succinimide).

Disease	Sample type	Transducer	Sensor/electrode material	Surface modification	Receptor	Target	Sensitivity	Turnaround time	Refs.
SARS-CoV-2	Fingerstick blood Serum of venous blood Plasma of venous blood	Optical	NC membrane	AuNP conjugates	SARS-CoV-2 spike protein	Anti-SARS-CoV-2 IgG/IgM	88.66% along with a specificity of 90.63%	15 min	[25]
ZIKV	Serum Saliva	Electrochemical	SPCEs	Carbon support material	ΔNS1 Protein EDIII Protein	Anti- ZIKV IgG/IgM	17 fg mL^{-1} 53 fg mL^{-1}	1.5 h	[174]
SARS-CoV-2	Serum	Optical	NC membrane	LNPs	M-HIgG (RIgG)	Anti-SARS-CoV-2 IgG	N/A	10 min	[175]
Hepatitis-B	Serum	Electrochemical	SPCEs	AuNPs	HBsAg captured on the surface of magnetic beads	Anti-Hepatitis B IgG	3 mIU mL^{-1}	6 min	[177]
Inflammation	Serum	Optical	Si	Oxidized glutathione 3-ADMS EDC/NHS	Antibodies	IL-6 PCT CRP	1.05 pg mL^{-1} 10.64 pg mL^{-1} 29.4 pg mL^{-1}	<1.5 h	[190]
Inflammation	Serum	Optical	Glass/PDMS	AuNPs	Antibodies	Cytokines	5–20 pg mL^{-1}	40 min	[192]
Inflammation	Spiked cytokines in mouse serum	Electrochemical	GO	Oxidation	Antibodies	Cytokines	5 pg mL^{-1}	40 min	[193]

3.4. Multiplexed Biosensors for the Detection of Various Biomolecule Classes

Most of the biosensing platforms discussed so far have included single-analyte biosensors for the diagnosis of viral infections. Even the featured multianalyte biosensors are only capable of measuring different analytes of a single biomolecule class, but what is scarcely observed are multiplexed biosensors that can gauge different biomolecule classes simultaneously (such as surface proteins of pathogens, viral nucleic acids, inflammatory biomarkers, and/or IgG/IgM antibodies). Although more infrequent, there are some emerging efforts to remedy this (**Table 4**).

As previously mentioned, recently, a graphene electrode-based portable RapidPlex biosensor enabled the detection of multiple COVID-19 biomarkers (N protein for diagnosis, SARS-CoV-2-specific IgG and IgM antibody isotypes for screening the immune response, and inflammatory biomarker C-reactive protein for disease severity) in saliva and blood samples by parallel measurements along with superior sensitivity and selectivity.[107]

Similarly, in an exciting application of the current optofluidic systems discussed thus far, liquid-core and solid-core ARROWs were intersected for planar fluorescence excitation and detection of Zika virus NS1 protein or a specific section of the Zika genome.[195] This study first introduced optofluidic wavelength division multiplexing using MMI photonic platform. Along the waveguide, there is constructive interference that occurs at well-defined lengths, which create different images of fluorescently captured Zika virus molecules. Under pressure-driven flow, the targets are excited and detected with orthogonally aligned liquid-core ARROW and MMI coupled to a collection solid-core waveguide. Fluorescent signals from either nucleic acid or NS1 protein isolation and detection were quantified with distinct peak profiles. Although these studies were performed with the commercially available target nucleic acid and target recombinant NS1 protein, this technique yields excellent innovation and promise for dual detection of viral nucleic acids and direct detection of viral antigens from a single sample. Given that this technology utilized standard streptavidin-coated micro-spheres for target nucleic acid and protein capture, further studies should be executed to assess the platform's sensitivity in the presence of clinical samples where there is a more tremendous potential for cross-reactivity or nonspecific binding.
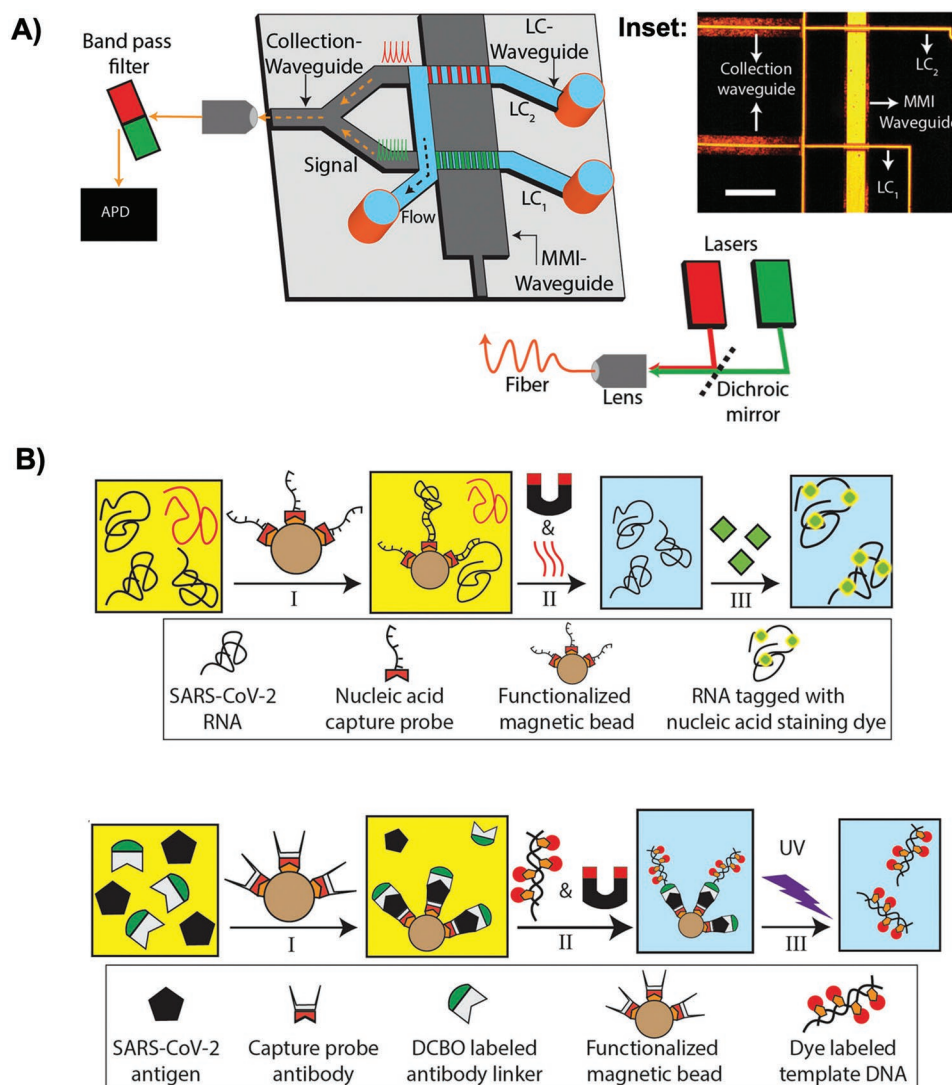
For furthering the simultaneous aspiration detection of nucleic acids and antigen proteins, studies include techniques such as ARROW, MMI, and fluorescent probe detection of viral nucleic acid and antigens unified with different forms of liquid-core, collection, solid-core waveguides for simultaneous multiplexed detection of SARS-CoV-2 RNA and N protein from the same spiked nasopharyngeal swab sample.[196] Building upon the previous technology,[94,150,195] nucleic acid capture probes were utilized for SARS-CoV-2 RNA trapping, and detection with a nucleic acid staining dye SARS-CoV-2 N protein was detected at a single molecule level employing a reporter-based Cy-5 DNA probe. Quantification of RNA or single protein was evaluated with continuous-wavelength-transform analysis, which considers fluorescent trace events as peaks or counts over time. Although these experiments express a LOD within the attomolar range for nucleic acids and a LOD of 0.7 ng mL^{-1} for antigens, these experiments were carried out only with clinically relevant concentrations of RNA and N protein spiked nasopharyngeal samples. It would be interesting to observe the sensitivity of the multiplexed, simultaneous detection of RNA and antigen with clinical samples (**Figure 11**). Therefore, more platforms that allow combinatorial detection of target analytes should be developed to evaluate a particular disease from diverse perspectives.

4. Conclusion and Future Perspectives

Indirect virus detection, for example using commercial PCR-based devices, is still the current gold standard in clinical settings since it provides a very high sensitivity and selectivity. However, this approach requires an extensive sample preparation, including lysis, purification, and reverse transcription, in order to obtain the genetic material to be analyzed, and bulky and

Table 4. Multiplexed biosensors for the detection of various biomolecule classes upon viral infection (SARS-CoV-2: severe acute respiratory syndrome coronavirus 2, PBA: 1-pyrenebutyric acid, NP: nucleocapsid protein, CRP: C-reactive protein, IgG: immunoglobulin G antibody, IgM: immunoglobulin M antibody, S1: spike protein; ZIKV: Zika virus, PBS: phosphate buffered saline, MMI: multimode interference, ARROW: assay antiresonant reflecting optical waveguides, NS1: nucleocapsid protein, N: nucleocapsid).

Disease	Sample Type	Transducer	Sensor/electrode material	Surface modification	Receptor	Target	Sensitivity	Turnaround time	Refs.
SARS-CoV-2	Fingerstick blood Saliva	Electrochemical	Graphene	PBA linker	Anti-SARS-CoV-2 Ab Anti-CRP Ab SARS-CoV-2 S1 protein	SARS-CoV-2 NP CRP IgG and IgM	N/A	1–10 min	[107]
Zika virus	PBS	Optical	MMI ARROW chip	Streptavidin-coated microspheres	Complementary ZIKV target nucleic acid Anti-ZIKV-NS1 antibody	ZIKV target nucleic acid ZIKV-NS1 protein	N/A	2–3 h	[195]
SARS-CoV-2	Nasopharyngeal swabs	Optical	ARROW chip	Streptavidin-coated magnetic beads	Complementary SARS-CoV-2 N gene sequence Anti-SARS-CoV-2 N antigen	N gene SARS-CoV-2 N antigen	2.1×10^{-3} PFU mL^{-1} 0.7 ng mL^{-1}	2 h	[196]

**ADVANCED
SCIENCE NEWS**

www.advancedsciencenews.com

**ADVANCED
MATERIALS**

www.advmat.de

Figure 11. Dual-target analysis of SARS-CoV-2 RNA (N gene) and N protein antigen. A) Cartoon layout of the single-molecule optofluidic chip design which features the ARROW biosensor chip and direction of flow of fluids and light (dashed lines). The inset describes a top-down optical image of the ARROW biosensor (scale: 200 μm) B) Assay steps for dual-target analysis. Top: i) SARS-CoV-2 RNA targets spiked in nasopharyngeal swabs bind complementary to the nucleic acid probe functionalized magnetic bead. ii) Washing of excess magnetic beads and unbound non-specific molecules with thermal release of captured RNAs. iii) Captured target RNAs are detected when tagged with fluorescent nucleic acid staining dye. Bottom: i) SARS-CoV-2 antigens are spiked into nasopharyngeal swabs and tagged with a diarylcyclooctyne moiety (DBCO) by click chemistry to form a DBCO–antibody–antigen complex. ii) Target antigens are then tagged with fluorescently labeled template DNA reporter probes and washing of excess magnetic beads and unbound non-specific molecules are washed off. iii) DNA reported probes have photocleavable azide and captured probes are cleaved off the beads with UV exposure and eluted for detection. A,B) Reproduced with permsission.[196] Copyright 2021, AIP Publishing. This article is distributed under a Creative Commons Attribution (CC BY) license.

expensive instruments as well as skilled personnel. Due to the multiple thermocycling steps needed, it is highly challenging to adapt PCR-based methods into biosensing technologies. Only a few promising examples currently exist.[126] In order to overcome these issues, several isothermal amplification strategies such as RPA or LAMP were combined with biosensors, where we saw during this pandemic for first time their successful implementation as commercially available products, even for at-home use: Lucira COVID-19 All-In-One Test Kit[197] and Cue COVID-19.[198] A very promising approach for indirect virus detection is provided by the CRISPR/Cas technology,

enabling a single-step and target amplification-free detection. However, these approaches are not matured yet for a commercialized use.

On the other hand, biosensing approaches (such as LFAs, other optical and electrochemical biosensors) for the direct virus detection offer fast sample-to-result time (generally within 15 min), but have low sensitivity and reliability, especially at early disease stages when the viral load is low. Therefore, there is still a great and urgent demand for investigating on different research areas highly sensitive but also easy-to-use and low-cost approaches. Besides, the specificity of these type of biosensors is

limited compared to indirect approach since the biorecognition elements used (i.e., antibodies) are specific to the surface proteins. Therefore, their use for detecting virus mutations could be highly problematic (depending on where the mutation occurs) and should be continuously evaluated. To address this issue, artificial bioreceptors like aptamers or MIPs could be employed either to target the whole virus structure or could be easily and rapidly adapted to the new variants.

The third class of biosensors deals with the body's immune response upon a viral infection (for example, targeting serological or inflammation biomarkers) and thus, are mainly used as complementary diagnostic tools along with to the first two biosensor classes.[199] While the detection of antibodies indicates a response to viral infections (IgM) or the immunity against a virus (IgG), the quantification of proinflammatory cytokines and chemokines can be used to monitor the immune response and predict the disease pattern.

Considering the factors that inhibited the efficient management of the current COVID-19 pandemic, we have thoroughly evaluated the paucity of the clinical diagnostic methods applied to detect viral infections. To overcome this deficit in the clinical settings and beyond while providing better disease management for such pandemic situations, biosensors own superior features over traditional assays or methods: i) low costs, ii) short turnaround times, iii) high analytical performance (i.e., sensitivity and selectivity), iv) adaptability for multiplexing, parallelization, and v) POC testing. Thus, biosensing technologies are emerging as a feasible alternative for detecting viral infections.

However, while biosensors successfully address some of the significant bottlenecks of conventional assay systems, many are not reached the technology readiness level required for possible commercialization. Especially in terms of their scalability via mass production to provide the considerable number of tests needed in a pandemic, it is still one of the major issues. Other problems restricting the speed up the implementation and commercialization of biosensors for viral infectious disease management can be summarized as follows: i) resource-intensive and expensive development and production of biorecognition elements used to construct biosensors that can be replaced by synthetic biology made receptors, ii) the requirement of multiple sample collection, pre-treatment and (target and/or signal) amplification procedures performed using distinct devices or by manual handling instead of an fully integrated and automated all-in-one systems, iii) the need for laborious instrumentation or portable but costly equipment only enabling (semi)professional usage, iv) critical biosafety issues arising from active viral compound detection, v) sufficient data interpretation and readability that can be solved by integration of smart devices (such as tablets, smartphones) that would simplify sophisticated soft- and hardware for signal readout and analysis as well as enable data transmission[13,67,68] via Internet-of-Things (IoT) integration.[69,71] Further advancements could be achieved with decentralization, enhancing data security by eliminating third parties (i.e., centralized laboratories and institutions). Many biosensing platforms developed are still allowing single analyte detection but are not eligible for multiplexing. However, for proper disease management, it is crucial to measure the presence of a viral pathogen and (semi)continuously monitor the immune response-related biomarkers. Only with such an approach would it be possible to get the whole picture.

Another important issue is the monitoring of the viral load in order to understand how the infection of a patient is progressing. Herein, optofluidic biosensors are highly promising examples for clinical and POC diagnostics. They allow for testing low-level viral loads (aM–fM levels) in less than an hour and are capable of miniaturization and multiplexing. Thus, in future, optofluidic biosensors could be used for effective diagnostics of viral infectious diseases even at the pre-symptomatic stage.[94,151,199]

The emerging wearable (bio)sensors, in addition to their POC counterparts, will also play an essential role shortly.[200] During the current pandemic, we have already experienced the early applications of wearable devices like smartwatches and facemasks to detect asymptomatic and presymptomatic cases of COVID-19. Significantly, the great potential and feasibility of facemasks integrated with biosensors have been recently introduced for wearable COVID-19 detection when combined with synthetic biology. Using an origami-based sample collection and preparation unit, including an isothermal target and subsequent CRISPR-powered signal amplification, it was possible to detect SARS-CoV-2 viral RNA fragments on a conventional LFA within 90 minutes.[201] Hence, the extension of such unique wearable platforms, including the electrochemical ones,[202] for the noninvasive (and preferably multiplexed) detection and monitoring of other infectious diseases and/or immune response-related biomarkers (such as inflammation markers) would be a viable option for the management of such pandemic situations and hold the future of biosensing research.

The quantification and screening of whole viruses, virus-specific or host immune response biomarkers enable differentiative diagnosis, immune surveillance, allowing better disease management. Moreover, with the help of synthetic biology-powered biorecognition and signal enhancement, advanced materials and sensing approaches, the biosensing technology holds the promise of becoming a powerful tool for decentralized and democratized POC testing of pathogens with high analytical performance, especially supporting the diagnosis of viral infections when in low-resource settings.

Acknowledgements

Conflict of Interest

The authors declare no conflict of interest.

Keywords

[1] K. Shinya, M. Ebina, S. Yamada, M. Ono, N. Kasai, Y. Kawaoka, *Nature* **2006**, *440*, 435.

[2] D. Baud, D. J. Gubler, B. Schaub, M. C. Lanteri, D. Musso, *Lancet* **2017**, *390*, 2099.

[3] K. Dhama, S. Khan, R. Tiwari, S. Sircar, S. Bhat, Y. S. Malik, K. P. Singh, W. Chaicumpa, D. K. Bonilla-Aldana, A. J. Rodriguez-Morales, *Clin. Microbiol. Rev.* **2020**, 33, e00028.

[4] H. Feldmann, S. Jones, H.-D. Klenk, H.-J. Schnittler, *Nat. Rev. Immunol.* **2003**, *3*, 677.

[5] B. Rehermann, M. Nascimbeni, *Nat. Rev. Immunol.* **2005**, *5*, 215.

[6] P. Zhou, X.-L. Yang, X.-G. Wang, B. Hu, L. Zhang, W. Zhang, H.-R. Si, Y. Zhu, B. Li, C.-L. Huang, H.-D. Chen, J. Chen, Y. Luo, H. Guo, R.-D. Jiang, M.-Q. Liu, Y. Chen, X.-R. Shen, X. Wang, X.-S. Zheng, K. Zhao, Q.-J. Chen, F. Deng, L.-L. Liu, B. Yan, F.-X. Zhan, Y.-Y. Wang, G.-F. Xiao, Z.-L. Shi, *Nature* **2020**, *579*, 270.

[7] C. Drosten, S. Günther, W. Preiser, S. van der Werf, H.-R. Brodt, S. Becker, H. Rabenau, M. Panning, L. Kolesnikova, R. A. M. Fouchier, A. Berger, A.-M. Burguière, J. Cinatl, M. Eickmann, N. Escriou, K. Grywna, S. Kramme, J.-C. Manuguerra, S. Müller, V. Rickerts, M. Stürmer, S. Vieth, H.-D. Klenk, A. D. M. E. Osterhaus, H. Schmitz, H. W. Doerr, *N. Engl. J. Med.* **2003**, *348*, 1967.

[8] A. M. Zaki, S. van Boheemen, T. M. Bestebroer, A. D. M. E. Osterhaus, R. A. M. Fouchier, *N. Engl. J. Med.* **2012**, *367*, 1814.

[9] World Health Organization, "WHO Coronavirus (COVID-19) Dashboard," can be found under https://covid19.who.int, 2020.

[10] B. D. Kevadiya, J. Machhi, J. Herskovitz, M. D. Oleynikov, W. R. Blomberg, N. Bajwa, D. Soni, S. Das, M. Hasan, M. Patel, A. M. Senan, S. Gorantla, J. McMillan, B. Edagwa, R. Eisenberg, C. B. Gurumurthy, S. P. M. Reid, C. Punyadeera, L. Chang, H. E. Gendelman, *Nat. Mater.* **2021**, *20*, 593.

[11] N. Castaño, S. C. Cordts, M. Kurosu Jalil, K. S. Zhang, S. Koppaka, A. D. Bick, R. Paul, S. K. Y. Tang, *ACS Omega* **2021**, *6*, 6509.

[12] R. Subramanian, Q. He, M. Pascual, *Proc. Natl. Acad. Sci. USA* **2021**, *118*, e2019716118.

[13] S. Mavrikou, G. Moschopoulou, V. Tsekouras, S. Kintzios, *Sensors* **2020**, *20*, 3121.

[14] C. Dincer, R. Bruch, E. Costa-Rama, M. T. Fernández-Abedul, A. Merkoçi, A. Manz, G. A. Urban, F. Güder, *Adv. Mater.* **2019**, *31*, 1806739.

[15] P. J. Rosenthal, *Am. J. Trop. Med. Hyg.* **2020**, *102*, 915.

[16] Z. Shen, Y. Xiao, L. Kang, W. Ma, L. Shi, L. Zhang, Z. Zhou, J. Yang, J. Zhong, D. Yang, L. Guo, G. Zhang, H. Li, Y. Xu, M. Chen, Z. Gao, J. Wang, L. Ren, M. Li, *Clin. Infect. Dis.* **2020**, *71*, 713.

[17] M. Valassina, A. M. Cuppone, M. G. Cusi, P. E. Valensin, *Clin. Diagn. Virol.* **1997**, *8*, 227.

[18] A. Tahamtan, A. Ardebili, *Expert Rev. Mol. Diagn.* **2020**, *20*, 453.

[19] J. D. Robin, A. T. Ludlow, R. LaRanger, W. E. Wright, J. W. Shay, *Sci. Rep.* **2016**, *6*, 24067.

[20] G. M. Ke, H. L. Cheng, L. Y. Ke, W. T. Ji, J. L. C. Chulu, M. H. Liao, T. J. Chang, H. J. Liu, *J. Virol. Methods* **2006**, *133*, 6.

[21] J. D. Diaz-Decaro, N. M. Green, H. A. Godwin, *Expert Rev. Mol. Diagn.* **2018**, *18*, 631.

[22] R. Weissleder, H. Lee, J. Ko, M. J. Pittet, *Sci. Transl. Med.* **2020**, *12*, eabc1931.

[23] J. B. Nuzzo, *Health Secur.* **2017**, *15*, 17.

[24] W. Zhang, B. D. Davis, S. S. Chen, J. M. Sincuir Martinez, J. T. Plummer, E. Vail, *J. Am. Med. Assoc.* **2021**, *325*, 1324.

[25] Z. Li, Y. Yi, X. Luo, N. Xiong, Y. Liu, S. Li, R. Sun, Y. Wang, B. Hu, W. Chen, Y. Zhang, J. Wang, B. Huang, Y. Lin, J. Yang, W. Cai, X. Wang, J. Cheng, Z. Chen, K. Sun, W. Pan, Z. Zhan, L. Chen, F. Ye, *J. Med. Virol.* **2020**, *92*, 1518.

[26] D. Sterlin, A. Mathian, M. Miyara, A. Mohr, F. Anna, L. Claër, P. Quentric, J. Fadlallah, H. Devilliers, P. Ghillani, C. Gunn, R. Hockett, S. Mudumba, A. Guihot, C.-E. Luyt, J. Mayaux, A. Beurton, S. Fourati, T. Bruel, O. Schwartz, J.-M. Lacorte, H. Yssel, C. Parizot, K. Dorgham, P. Charneau, Z. Amoura, G. Gorochov, *Sci. Transl. Med.* **2021**, *13*, eabd2223.

[27] Y. Galipeau, M. Greig, G. Liu, M. Driedger, M.-A. Langlois, *Front. Immunol.* **2020**, *11*, 610688.

[28] L. Cinquanta, D. E. Fontana, N. Bizzaro, *Autoimmun. Highlights* **2017**, *8*, 9.

[29] M. F. Clark, R. M. Lister, M. Bar-Joseph, ELISA techniques, *Methods Enzymol.* **1986**, *118*, 742.

[30] K. M. Koczula, A. Gallotta, *Essays Biochem.* **2016**, *60*, 111.

[31] J. D. Whitman, J. Hiatt, C. T. Mowery, B. R. Shy, R. Yu, T. N. Yamamoto, U. Rathore, G. M. Goldgof, C. Whitty, J. M. Woo, A. E. Gallman, T. E. Miller, A. G. Levine, D. N. Nguyen, S. P. Bapat, J. Balcerek, S. A. Bylsma, A. M. Lyons, S. Li, A. W. Wong, E. M. Gillis-Buck, Z. B. Steinhart, Y. Lee, R. Apathy, M. J. Lipke, J. A. Smith, T. Zheng, I. C. Boothby, E. Isaza, J. Chan, et al., *Nat. Biotechnol.* **2020**, *38*, 1174.

[32] C. for D. and R. Health, "Coronavirus Disease 2019 (COVID-19) Emergency Use Authorizations for Medical Devices," can be found under https://www.fda.gov/medical-devices/emergency-use-authorizations-medical-devices/coronavirus-disease-2019-covid-19-emergency-use-authorizations-medical-devices, 2021.

[33] M. J. Mina, R. Parker, D. B. Larremore, *N. Engl. J. Med.* **2020**, *383*, e120.

[34] T. Ji, Z. Liu, G. Wang, X. Guo, S. Akbar khan, C. Lai, H. Chen, S. Huang, S. Xia, B. Chen, H. Jia, Y. Chen, Q. Zhou, *Biosens. Bioelectron.* **2020**, *166*, 112455.

[35] N. Bhalla, P. Jolly, N. Formisano, P. Estrela, *Essays Biochem.* **2016**, *60*, 1.

[36] D. O'Hare, in Biosensors and Sensor Systems. *Body Sensor Networks* (Ed: G.-Z. Yang), Springer, 2nd Ed., London, **2014**, pp. 55–115.

[37] B. N. Johnson, R. Mutharasan, *Analyst* **2014**, *139*, 1576.

[38] M. Ritzi-Lehnert, *Expert Rev. Mol. Diagn.* **2012**, *12*, 189.

[39] X. Hou, Y. S. Zhang, G. T. Santiago, M. M. Alvarez, J. Ribas, S. J. Jonas, P. S. Weiss, A. M. Andrews, J. Aizenberg, A. Khademhosseini, *Nat. Rev. Mater.* **2017**, *2*, 17016.

[40] H. A. Alhadrami, *Biotechnol. Appl. Biochem.* **2018**, *65*, 497.

[41] B. Purohit, P. R. Vernekar, N. P. Shetti, P. Chandra, *Sens. Int.* **2020**, *1*, 100040.

[42] S. M. Yoo, S. Y. Lee, *Trends Biotechnol.* **2016**, *34*, 7.

[43] H. Nguyen, J. Park, S. Kang, M. Kim, *Sensors* **2015**, *15*, 10481.

[44] N. S. Ferreira, M. G. F. Sales, *Biosens. Bioelectron.* **2014**, *53*, 193.

[45] P. Leonard, S. Hearty, J. Brennan, L. Dunne, J. Quinn, T. Chakraborty, R. O'Kennedy, *Enzyme Microb. Technol.* **2003**, *32*, 3.

[46] G. Papadakis, P. Murasova, A. Hamiot, K. Tsougeni, G. Kaprou, M. Eck, D. Rabus, Z. Bilkova, B. Dupuy, G. Jobst, A. Tserepi, E. Gogolides, E. Gizeli, *Biosens. Bioelectron.* **2018**, *111*, 52.

[47] M. Megens, M. Prins, *J. Magn. Magn. Mater.* **2005**, *293*, 702.

[48] K. Ramanathan, B. Danielsson, *Biosens. Bioelectron.* **2001**, *16*, 417.

[49] A. Hlaváček, M. J. Mickert, T. Soukka, S. Lahtinen, T. Tallgren, N. Pizúrová, A. Król, H. H. Gorris, *Anal. Chem.* **2019**, *91*, 1241.

[50] H. Malekzad, P. Sahandi Zangabad, H. Mirshekari, M. Karimi, M. R. Hamblin, *Nanotechnol. Rev.* **2017**, *6*, 301.

[51] M. Holzinger, A. Le Goff, S. Cosnier, *Front. Chem.* **2014**, *2*.

[52] E. Heydari-Bafrooei, A. A. Ensafi, in *Electrochemical Biosensors*, (Ed: A. A. Ensafi), Elsevier, Amsterdam **2019**, pp. 77–98, https://doi.org/10.1016/B978-0-12-816491-4.00004-8.

[53] N. Sandhyarani, in. *Electrochemical Biosensors*, (Ed: A. A. Ensafi), Elsevier, Amsterdam **2019**, pp. 45–75, https://doi.org/10.1016/B978-0-12-816491-4.00003-6.

[54] J. Lei, H. Ju, *Chem. Soc. Rev.* **2012**, *41*, 2122.

[55] A. Rasooly, B. Prickril, *Biosensors and Biodetection: Methods and Protocols Volume 1: Optical-Based Detectors*, Humana Press, New York, Methods in Molecular Biology, 1st Ed., **2009**, *501*, 472.

[56] V. Perumal, U. Hashim, Advances in biosensors: Principle, architecture and applications, *J. Appl. Biomed.* **2014**, *12*, 1

[57] M. Zourob, *Recognition Receptors in Biosensors*, Springer, New York **2010**.

[58] O. Hayden, P. A. Lieberzeit, D. Blaas, F. L. Dickert, Artificial antibodies for bioanalyte detection—Sensing viruses and proteins, *Adv. Funct. Mater.* **2006**, *16*, 1269

[59] M. A. Morales, J. M. Halpern, *Bioconjugate Chem.* **2018**, *29*, 3231.

[60] F. M. Marty, K. Chen, K. A. Verrill, *N. Engl. J. Med.* **2020**, *382*, e76.

[61] A. A. Zasada, K. Zacharczuk, K. Woźnica, M. Główka, R. Ziółkowski, E. Malinowska, *AMB Express* **2020**, *10*, 46.

[62] N. Bunyakul, A. Baeumner, *Sensors* **2014**, *15*, 547.

[63] K. D. Clark, C. Zhang, J. L. Anderson, *Anal. Chem.* **2016**, *88*, 11262.

[64] Spindiag, "Rhonda SARS COV-2 disk," can be found under https://www.spindiag.de/sars-cov-2-disk/, **2021**.

[65] A. Ferrand, K. D. Schleicher, N. Ehrenfeuchter, W. Heusermann, O. Biehlmaier, *Sci. Rep.* **2019**, *9*, 1165.

[66] M. Shokrekhodaei, S. Quinones, Z. Fazel, H. Nazeran, *Adv. Electr. Electron. Eng.* **2019**, *17*, 64.

[67] Y.-D. Ma, K.-H. Li, Y.-H. Chen, Y.-M. Lee, S.-T. Chou, Y.-Y. Lai, P.-C. Huang, H.-P. Ma, G.-B. Lee, *Lab Chip* **2019**, *19*, 3804.

[68] A. Priye, C. S. Ball, R. J. Meagher, *Anal. Chem.* **2018**, *90*, 12385.

[69] S. Jain, M. Nehra, R. Kumar, N. Dilbaghi, T. Hu, S. Kumar, A. Kaushik, C. Li, *Biosens. Bioelectron.* **2021**, *179*, 113074.

[70] M. Mayer, A. J. Baeumner, *Chem. Rev.* **2019**, *119*, 7996.

[71] A. Altay, R. Learney, F. Güder, C. Dincer, *Trends Biotechnol.* **2022**, *40*, 141.

[72] J. C. Huang, Y.-F. Chang, K.-H. Chen, L.-C. Su, C.-W. Lee, C.-C. Chen, Y.-M. A. Chen, C. Chou, *Biosens. Bioelectron.* **2009**, *25*, 320.

[73] X. Che, L. Qiu, Y. Pan, K. Wen, W. Hao, L. Zhang, Y. Wang, Z. Liao, X. Hua, V. C. C. Cheng, K. Yuen, *J. Clin. Microbiol.* **2004**, *42*, 2629.

[74] B. Yang, H. Gong, C. Chen, X. Chen, C. Cai, *Biosens. Bioelectron.* **2017**, *87*, 679.

[75] B. Zuo, S. Li, Z. Guo, J. Zhang, C. Chen, *Anal. Chem.* **2004**, *76*, 3536.

[76] F. Patolsky, G. Zheng, O. Hayden, M. Lakadamyali, X. Zhuang, C. M. Lieber, *Proc. Natl. Acad. Sci. USA* **2004**, *101*, 14017.

[77] V. D. Krishna, K. Wu, A. M. Perez, J.-P. Wang, *Front. Microbiol.* **2016**, *7*, 1.

[78] R. Vainionpää, P. Leinikki, in *Encyclopedia of Virology*, (Eds: B. W. J. Mahy, M. H. V. Van Regenmortel), *3*, Elsevier, Amsterdam **2008**, pp. 29–37, https://doi.org/10.1016/B978-012374410-4.00585-9.

[79] A. Sinha, R. Lutter, T. Dekker, B. Dierdorp, P. J. Sterk, U. Frey, E. Delgado-Eckert, *Viruses* **2020**, *12*, 1175.

[80] B. O'Farrell, in Evolution in Lateral Flow–Based Immunoassay Systems. (Eds: R. Wong, H. Tse), *Lateral Flow Immunoassay*, Humana Press, Totowa, NJ **2009**, pp. 1–33, https://doi.org/10.1007/978-1-59745-240-3_1.

[81] T. Peto, D. Affron, B. Afrough, A. Agasu, M. Ainsworth, A. Allanson, K. Allen, C. Allen, L. Archer, N. Ashbridge, I. Aurfan, M. Avery, E. Badenoch, P. Bagga, R. Balaji, E. Baldwin, S. Barraclough, C. Beane, J. Bell, T. Benford, S. Bird, M. Bishop, A. Bloss, R. Body, R. Boulton, A. Bown, C. Bratten, C. Bridgeman, D. Britton, T. Brooks, et al., *EClinicalMedicine* **2021**, *36*, 100924.

[82] Y. Pan, L. Long, D. Zhang, T. Yuan, S. Cui, P. Yang, Q. Wang, S. Ren, *Clin. Chem.* **2020**, *66*, 794.

[83] J. Ziebuhr, *Curr. Top. Microbiol. Immunol.* **2005**, *287*, 57.

[84] P. S. Masters, *Virology* **2019**, *537*, 198.

[85] G. Seo, G. Lee, M. J. Kim, S.-H. Baek, M. Choi, K. B. Ku, C.-S. Lee, S. Jun, D. Park, H. G. Kim, S. I. S.-J. Kim, J.-O. Lee, B. T. Kim, E. C. Park, S. I. S.-J. Kim, *ACS Nano* **2020**, *14*, 5135.

[86] Y. Sun, Y. Bai, D. Song, X. Li, L. Wang, H. Zhang, *Biosens. Bioelectron.* **2007**, *23*, 473.

[87] E. Kretschmann, H. Raether, *Z. Naturforsch. A* **1968**, *23*, 2135.

[88] A. A. Yanik, M. Huang, O. Kamohara, A. Artar, T. W. Geisbert, J. H. Connor, H. Altug, *Nano Lett.* **2010**, *10*, 4962.

[89] T. J. Park, M. S. Hyun, H. J. Lee, S. Y. Lee, S. Ko, *Talanta* **2009**, *79*, 295.

[90] R. C. Stringer, S. Schommer, D. Hoehn, S. A. Grant, *Sens. Actuators, B* **2008**, *134*, 427.

[91] L. Mockus, J. J. Peterson, J. M. Lainez, G. V. Reklaitis, *Org. Process Res. Dev.* **2015**, *19*, 908.

[92] J. Nette, P. D. Howes, A. J. DeMello, *Adv. Mater. Technol.* **2020**, *5*, 2000060.

[93] A. J. DeMello, *Nature* **2006**, *442*, 394.

[94] A. Stambaugh, J. W. Parks, M. A. Stott, G. G. Meena, A. R. Hawkins, H. Schmidt, *Proc. Natl. Acad. Sci. USA* **2021**, *118*, 2.

[95] X. Yang, C. Gong, Y. Liu, Y. Rao, M. Smietana, Y. Gong, *Photonic Sens.* **2021**, *11*, 262

[96] L. He, S. K. Ozdemir, J. Zhu, W. Kim, L. Yang, *Nat. Nanotechnol.* **2011**, *6*, 428.

[97] Y. Liu, X. Zhang, *Micromachines* **2021**, *12*, 826.

[98] Y. Zhang, Y. Zhao, T. Zhou, Q. Wu, *Lab Chip* **2018**, *18*, 57.

[99] J. E. Baker, R. Sriram, B. L. Miller, *Lab Chip* **2017**, *17*, 1570.

[100] Z. Fu, Y.-C. Lu, J. J. Lai, *Chonnam Med. J.* **2019**, *55*, 86.

[101] S. Esposito, A. Mencacci, E. Cenci, B. Camilloni, E. Silvestri, N. Principi, *Front. Cell. Infect. Microbiol.* **2019**, *9*.

[102] J. Li, J. Macdonald, *Biosens. Bioelectron.* **2016**, *83*, 177.

[103] National Center for Immunization and Respiratory Diseases (NCIRD), Division of Viral Diseases, "CDC's Influenza SARS-CoV-2 Multiplex Assay and Required Supplies," can be found under https://www.cdc.gov/coronavirus/2019-ncov/lab/multiplex.html, **2020**.

[104] R. D. Blevins, R. Plunkett, *J. Appl. Mech.* **1980**, *47*, 461.

[105] D. Ozcelik, J. W. J. W. Parks, T. A. Wall, M. A. Stott, H. Cai, J. W. J. W. Parks, A. R. Hawkins, H. Schmidt, *Proc. Natl. Acad. Sci. USA* **2015**, *112*, 12933.

[106] Y. Shi, K. T. Nguyen, L. K. Chin, Z. Li, L. Xiao, H. Cai, R. Yu, W. Huang, S. Feng, P. H. Yap, J. Liu, Y. Zhang, A. Q. Liu, *ACS Sens.* **2021**, *6*, 3445.

[107] R. M. Torrente-Rodríguez, H. Lukas, J. Tu, J. Min, Y. Yang, C. Xu, H. B. Rossiter, W. Gao, *Matter* **2020**, *3*, 1981

[108] M. D. T. Torres, W. R. de Araujo, L. F. de Lima, A. L. Ferreira, C. de la Fuente-Nunez, *Matter* **2021**, *4*, 2403

[109] L. Chen, X. Wang, W. Lu, X. Wu, J. Li, *Chem. Soc. Rev.* **2016**, *45*, 2137.

[110] S. Matsunaga, S. S. Jeremiah, K. Miyakawa, D. Kurotaki, S. Shizukuishi, K. Watashi, H. Nishitsuji, H. Kimura, T. Tamura, N. Yamamoto, K. Shimotohno, T. Wakita, A. Ryo, *iScience* **2020**, *23*, 100867.

[111] F. N. Ishikawa, H.-K. Chang, M. Curreli, H.-I. Liao, C. A. Olson, P.-C. Chen, R. Zhang, R. W. Roberts, R. Sun, R. J. Cote, M. E. Thompson, C. Zhou, *ACS Nano* **2009**, *3*, 1219.

[112] M. Jenik, R. Schirhagl, C. Schirk, O. Hayden, P. Lieberzeit, D. Blaas, G. Paul, F. L. Dickert, *Anal. Chem.* **2009**, *81*, 5320.

[113] World Health Organization, "Tracking SARS-CoV-2 variants," can be found under https://www.who.int/health-topics/typhoid/tracking-SARS-CoV-2-variants, **2021**.

**ADVANCED
SCIENCE NEWS**

www.advancedsciencenews.com

**ADVANCED
MATERIALS**

www.advmat.de

[114] K. Guo, S. Wustoni, A. Koklu, E. Díaz-Galicia, M. Moser, A. Hama, A. A. Alqahtani, A. N. Ahmad, F. S. Alhamlan, M. Shuaib, A. Pain, I. McCulloch, S. T. Arold, R. Grünberg, S. Inal, *Nat. Biomed. Eng.* **2021**, *5*, 666.

[115] A. D. Ellington, J. W. Szostak, *Nature* **1990**, *346*, 818.

[116] C. H. van den Kieboom, S. L. van der Beek, T. Mészáros, R. E. Gyurcsányi, G. Ferwerda, M. I. de Jonge, *TrAC, Trends Anal. Chem.* **2015**, *74*, 58.

[117] J. Labuda, A. M. O. Brett, G. Evtugyn, M. Fojta, M. Mascini, M. Ozsoz, I. Palchetti, E. Paleček, J. Wang, *Pure Appl. Chem.* **2010**, *82*, 1161

[118] C. Bai, Z. Lu, H. Jiang, Z. Yang, X. Liu, H. Ding, H. Li, J. Dong, A. Huang, T. Fang, Y. Jiang, L. Zhu, X. Lou, S. Li, N. Shao, *Biosens. Bioelectron.* **2018**, *110*, 162.

[119] J. Bhardwaj, N. Chaudhary, H. Kim, J. Jang, *Anal. Chim. Acta* **2019**, *1064*, 94.

[120] H.-C. Lai, C.-H. Wang, T.-M. Liou, G.-B. Lee, *Lab Chip* **2014**, *14*, 2002.

[121] D. K. W. Chu, Y. Pan, S. M. S. Cheng, K. P. Y. Hui, P. Krishnan, Y. Liu, D. Y. M. Ng, C. K. C. Wan, P. Yang, Q. Wang, M. Peiris, L. L. M. Poon, *Clin. Chem.* **2020**, *66*, 549.

[122] D. N. Fredricks, D. A. Relman, *Clin. Infect. Dis.* **1999**, *29*, 475.

[123] G. Heilek, in *Nucleic Acids – From Basic Aspects to Laboratory Tools* (Eds: M. L. Larramendy, S. Soloneski), InTech, London **2016**.

[124] M. G. Ghannam, M. Varacallo, Biochemistry, Polymerase Chain Reaction. [Updated 2021 May 9]. In: StatPearls [Internet]. Treasure Island (FL): StatPearls Publishing; **2022**. Available from: https://www.ncbi.nlm.nih.gov/books/NBK535453/

[125] L. Garibyan, N. Avashia, *J. Invest. Dermatol.* **2013**, *133*, 1.

[126] E. Nunez-Bajo, A. Silva Pinto Collins, M. Kasimatis, Y. Cotur, T. Asfour, U. Tanriverdi, M. Grell, M. Kaisti, G. Senesi, K. Stevenson, F. Güder, *Nat. Commun.* **2020**, *11*, 6176.

[127] J. P. Broughton, X. Deng, G. Yu, C. L. Fasching, V. Servellita, J. Singh, X. Miao, J. A. Streithorst, A. Granados, A. Sotomayor-Gonzalez, K. Zorn, A. Gopez, E. Hsu, W. Gu, S. Miller, C. Y. Pan, H. Guevara, D. A. Wadford, J. S. Chen, C. Y. Chiu, *Nat. Biotechnol.* **2020**, 38, 870.

[128] J. F.-W. Chan, C. C.-Y. Yip, K. K.-W. To, T. H.-C. Tang, S. C.-Y. Wong, K.-H. Leung, A. Y.-F. Fung, A. C.-K. Ng, Z. Zou, H.-W. Tsoi, G. K.-Y. Choi, A. R. Tam, V. C.-C. Cheng, K.-H. Chan, O. T.-Y. Tsang, K.-Y. Yuen, *J. Clin. Microbiol.* **2020**, *58*, e00310.

[129] E. Morales-Narváez, C. Dincer, *Biosens. Bioelectron.* **2020**, *163*, 112274.

[130] T. Chaibun, J. Puenpa, T. Ngamdee, N. Boonapatcharoen, P. Athamanolap, A. P. O'Mullane, S. Vongpunsawad, Y. Poovorawan, S. Y. Lee, B. Lertanantawong, *Nat. Commun.* **2021**, *12*, 802.

[131] P. Teengam, W. Siangproh, A. Tuantranont, T. Vilaivan, O. Chailapakul, C. S. Henry, *Anal. Chem.* **2017**, *89*, 5428.

[132] P. Fozouni, S. Son, M. Díaz de León Derby, G. J. Knott, C. N. Gray, M. V. D'Ambrosio, C. Zhao, N. A. Switz, G. R. Kumar, S. I. Stephens, D. Boehm, C.-L. Tsou, J. Shu, A. Bhuiya, M. Armstrong, A. R. Harris, P.-Y. Chen, J. M. Osterloh, A. Meyer-Franke, B. Joehnk, K. Walcott, A. Sil, C. Langelier, K. S. Pollard, E. D. Crawford, A. S. Puschnik, M. Phelps, A. Kistler, J. L. DeRisi, J. A. Doudna, et al., *Cell* **2020**, *184*, 323

[133] L. Zanoli, G. Spoto, *Biosensors* **2012**, *3*, 18.

[134] H. Kuhn, V. V. Demidov, M. D. Frank-Kamenetskii, *Nucleic Acids Res.* **2002**, *30*, 574.

[135] T. Notomi, T. Notomi, T. Okayama, H. Masubuchi, H. Yonekawa, T. Watanabe, K. Amino, N. Hase, *Nucleic Acids Res.* **2000**, *28*, 63e.

[136] X. Zhu, X. Wang, L. Han, T. Chen, L. Wang, H. Li, S. Li, L. He, X. Fu, S. Chen, M. Xing, H. Chen, Y. Wang, *Biosens. Bioelectron.* **2020**, *166*, 112437.

[137] I. M. Lobato, C. K. O'Sullivan, *TrAC, Trends Anal. Chem.* **2018**, *98*, 19.

[138] O. Behrmann, I. Bachmann, M. Spiegel, M. Schramm, A. Abd El Wahed, G. Dobler, G. Dame, F. T. Hufert, *Clin. Chem.* **2020**, *66*, 1047.

[139] B. Koo, C. E. Jin, T. Y. Lee, J. H. Lee, M. K. Park, H. Sung, S. Y. Park, H. J. Lee, S. M. Kim, J. Y. Kim, S.-H. Kim, Y. Shin, *Biosens. Bioelectron.* **2017**, *90*, 187.

[140] H. E. Kim, A. Schuck, S. H. Lee, Y. Lee, M. Kang, Y.-S. Kim, *Biosens. Bioelectron.* **2021**, *182*, 113168.

[141] R. J. Meagher, A. Priye, Y. K. Light, C. Huang, E. Wang, *Analyst* **2018**, *143*, 1924.

[142] J. C. Rolando, E. Jue, J. T. Barlow, R. F. Ismagilov, *Nucleic Acids Res.* **2020**, *48*, e42.

[143] I. Smyrlaki, M. Ekman, A. Lentini, N. Rufino de Sousa, N. Papanicolaou, M. Vondracek, J. Aarum, H. Safari, S. Muradrasoli, A. G. Rothfuchs, J. Albert, B. Högberg, B. Reinius, *Nat. Commun.* **2020**, *11*, 4812.

[144] H. Kutluk, R. Bruch, G. A. Urban, C. Dincer, *Biosens. Bioelectron.* **2020**, *148*, 111824.

[145] L. Shi, Q. Sun, J. He, H. Xu, C. Liu, C. Zhao, Y. Xu, C. Wu, J. Xiang, D. Gu, J. Long, H. Lan, *Biomed. Mater. Eng.* **2015**, *26*, S2207.

[146] G. Martínez-Paredes, M. B. González-García, A. Costa-García, *Electroanalysis* **2009**, *21*, 379.

[147] National Center for Immunization and Respiratory Diseases (NCIRD), Division of Viral Diseases, "SARS-CoV-2 Variant Classifications and Definitions," can be found under https://www.cdc.gov/coronavirus/2019-ncov/variants/variant-classifications.html, **2020**.

[148] W.-S. Choi, J. H. Jeong, H. D. G. Nicolas, S. Oh, K. J. C. Antigua, J.-H. Park, B. Kim, S.-W. Yoon, K. S. Shin, Y. K. Choi, Y. H. Baek, M.-S. Song, *Diagnostics* **2020**, *10*, 775.

[149] K. Du, H. Cai, M. Park, T. A. Wall, M. A. Stott, K. J. Alfson, A. Griffiths, R. Carrion, J. L. Patterson, A. R. Hawkins, H. Schmidt, R. A. Mathies, *Biosens. Bioelectron.* **2017**, *91*, 489.

[150] H. Cai, J. W. Parks, T. A. Wall, M. A. Stott, A. Stambaugh, K. Alfson, A. Griffiths, R. A. Mathies, R. Carrion, J. L. Patterson, A. R. Hawkins, H. Schmidt, *Sci. Rep.* **2015**, *5*, 14494.

[151] M. Makela, P. T. Lin, *Anal. Chem.* **2021**, *93*, 4154.

[152] J. D. Sander, J. K. Joung, *Nat. Biotechnol.* **2014**, *32*, 347.

[153] P. Mali, L. Yang, K. M. Esvelt, J. Aach, M. Guell, J. E. DiCarlo, J. E. Norville, G. M. Church, *Science* **2013**, *339*, 823.

[154] E. Senís, C. Fatouros, S. Große, E. Wiedtke, D. Niopek, A.-K. Mueller, K. Börner, D. Grimm, *Biotechnol. J.* **2014**, *9*, 1402.

[155] B. Chen, L. A. Gilbert, B. A. Cimini, J. Schnitzbauer, W. Zhang, G.-W. Li, J. Park, E. H. Blackburn, J. S. Weissman, L. S. Qi, B. Huang, *Cell* **2013**, *155*, 1479.

[156] H. Shinoda, Y. Taguchi, R. Nakagawa, A. Makino, S. Okazaki, M. Nakano, Y. Muramoto, C. Takahashi, I. Takahashi, J. Ando, T. Noda, O. Nureki, H. Nishimasu, R. Watanabe, *Commun. Biol.* **2021**, *4*, 476.

[157] A. Srivastava, S. Srivastava, D. J. Upadhyay, *Front. Mol. Biosci.* **2020**, *7*, 582499.

[158] F. Zhao, E. Y. Lee, G. S. Noh, J. Shin, H. Liu, Z. Qiao, Y. Shin, *Sci. Rep.* **2019**, *9*, 16374.

[159] R. Aman, A. Mahas, M. Mahfouz, *ACS Synth. Biol.* **2020**, *9*, 1226.

[160] M. Mehravar, A. Shirazi, M. M. Mehrazar, M. Nazari, M. Mehravar, M. Shirazi, A. Mehrazar, M. M. Nazari, *Avicenna J. Med. Biotechnol.* **2019**, *11*, 259.

[161] K. Pardee, A. A. Green, M. K. Takahashi, D. Braff, G. Lambert, J. W. Lee, T. Ferrante, D. Ma, N. Donghia, M. Fan, N. M. Daringer, I. Bosch, D. M. Dudley, D. H. O'Connor, L. Gehrke, J. J. Collins, *Cell* **2016**, *165*, 1255.

[162] L. Zhou, R. Peng, R. Zhang, J. Li, *J. Cell. Mol. Med.* **2018**, *22*, 5807.

[163] J.-H. Tsou, Q. Leng, F. Jiang, *Transl. Oncol.* **2019**, *12*, 1566.

[164] M. R. O'Connell, *J. Mol. Biol.* **2019**, *431*, 66.

[165] J. S. Gootenberg, O. O. Abudayyeh, J. W. Lee, P. Essletzbichler, A. J. Dy, J. Joung, V. Verdine, N. Donghia, N. M. Daringer, C. A. Freije, C. Myhrvold, R. P. Bhattacharyya, J. Livny, A. Regev, E. V. Koonin, D. T. Hung, P. C. Sabeti, J. J. Collins, F. Zhang, *Science* **2017**, *356*, 438.

[166] J. E. van Dongen, J. T. W. Berendsen, R. D. M. Steenbergen, R. M. F. Wolthuis, J. C. T. Eijkel, L. I. Segerink, *Biosens. Bioelectron.* **2020**, *166*, 112445.

[167] B. I. Escudero-Abarca, S. H. Suh, M. D. Moore, H. P. Dwivedi, L.-A. Jaykus, *PLoS One* **2014**, *9*, e106805.

[168] J. Kirkegaard, N. Rozlosnik, *Methods Mol. Biol.* **2017**, *1572*, 55.

[169] A. R. Fehr, R. Channappanavar, S. Perlman, *Annu. Rev. Med.* **2017**, *68*, 387.

[170] L. Qin, P. B. Gilbert, L. Corey, M. J. McElrath, S. G. Self, *J. Infect. Dis.* **2007**, *196*, 1304.

[171] W. Xu, D. Wang, D. Li, C. C. Liu, *Int. J. Mol. Sci.* **2019**, *21*, 134.

[172] R. Racine, G. M. Winslow, *Immunol. Lett.* **2009**, *125*, 79.

[173] S. Shukla, S.-Y. Hong, S. H. Chung, M. Kim, *Front. Microbiol.* **2016**, *7*, 1685.

[174] G. Cabral-Miranda, A. R. Cardoso, L. C. S. Ferreira, M. G. F. Sales, M. F. Bachmann, *Biosens. Bioelectron.* **2018**, *113*, 101.

[175] Z. Chen, Z. Zhang, X. Zhai, Y. Li, L. Lin, H. Zhao, L. Bian, P. Li, L. Yu, Y. Wu, G. Lin, *Anal. Chem.* **2020**, *92*, 7226.

[176] L. Pan, M. Mu, P. Yang, Y. Sun, R. Wang, J. Yan, P. Li, B. Hu, J. Wang, C. Hu, Y. Jin, X. Niu, R. Ping, Y. Du, T. Li, G. Xu, Q. Hu, L. Tu, *Am. J. Gastroenterol.* **2020**, *115*, 766.

[177] A. de la Escosura-Muñiz, M. Maltez-da Costa, C. Sánchez-Espinel, B. Díaz-Freitas, J. Fernández-Suarez, Á. González-Fernández, A. Merkoçi, *Biosens. Bioelectron.* **2010**, *26*, 1710.

[178] J. Highton, *Aust. N. Z. J. Med.* **1984**, *14*, 173.

[179] J. R. Dunkelberger, W.-C. Song, *Cell Res.* **2010**, *20*, 34.

[180] C. A. Janeway, R. Medzhitov, *Annu. Rev. Immunol.* **2002**, *20*, 197.

[181] D. Blanco-Melo, B. E. Nilsson-Payant, W.-C. Liu, S. Uhl, D. Hoagland, R. Møller, T. X. Jordan, K. Oishi, M. Panis, D. Sachs, T. T. Wang, R. E. Schwartz, J. K. Lim, R. A. Albrecht, B. R. TenOever, *Cell* **2020**, *181*, 1036.

[182] L. Berman, K. Hargreaves, in *Cohen's Pathways Pulp*, Elsevier, 12th Ed., Amsterdam **2020**, p. 928.

[183] T. Yusa, K. Tateda, A. Ohara, S. Miyazaki, *J. Infect. Chemother.* **2017**, *23*, 96.

[184] E. Terpos, I. Ntanasis-Stathopoulos, I. Elalamy, E. Kastritis, T. N. Sergentanis, M. Politou, T. Psaltopoulou, G. Gerotziafas, M. A. Dimopoulos, *Am. J. Hematol.* **2020**, *95*, 834.

[185] T. Herold, V. Jurinovic, C. Arnreich, B. J. Lipworth, J. C. Hellmuth, M. von Bergwelt-Baildon, M. Klein, T. Weinberger, *J. Allergy Clin. Immunol.* **2020**, *146*, 128.

[186] D. Ragab, H. Salah Eldin, M. Taeimah, R. Khattab, R. Salem, *Front. Immunol.* **2020**, *11*, 1446.

[187] N. Chen, M. Zhou, X. Dong, J. Qu, F. Gong, Y. Han, Y. Qiu, J. Wang, Y. Liu, Y. Wei, J. Xia, T. Yu, X. Zhang, L. Zhang, *Lancet* **2020**, *395*, 507.

[188] A. Gowri, N. Ashwin Kumar, B. S. Suresh Anand, *TrAC, Trends Anal. Chem.* **2021**, *137*, 116205.

[189] Y. Wang, J. Sun, Y. Hou, C. Zhang, D. Li, H. Li, M. Yang, C. Fan, B. Sun, *Biosens. Bioelectron.* **2019**, *141*, 111432.

[190] R. Nie, J. Huang, X. Xu, L. Yang, *Anal. Bioanal. Chem.* **2020**, *412*, 3231.

[191] K. M. Mayer, J. H. Hafner, *Chem. Rev.* **2011**, *111*, 3828.

[192] P. Chen, M. T. Chung, W. McHugh, R. Nidetz, Y. Li, J. Fu, T. T. Cornell, T. P. Shanley, K. Kurabayashi, *ACS Nano* **2015**, *9*, 4173.

[193] H. Wei, S. Ni, C. Cao, G. Yang, G. Liu, *ACS Sens.* **2018**, *3*, 1553.

[194] M. Garg, A. L. Sharma, S. Singh, *Biosens. Bioelectron.* **2021**, *171*, 112703.

[195] A. Stambaugh, J. W. Parks, M. A. Stott, G. G. Meena, A. R. Hawkins, H. Schmidt, *Biomed. Opt. Express* **2018**, *9*, 3725.

[196] G. G. Meena, A. M. Stambaugh, V. Ganjalizadeh, M. A. Stott, A. R. Hawkins, H. Schmidt, *APL Photonics* **2021**, *6*, 066101.

[197] U.S. Food and Drug Administration, Center for Devices and Radiological, U.S. Food and Drug Administration. https://www.fda.gov/medical-devices/coronavirus-covid-19-and-medical-devices/home-otc-covid-19-diagnostic-tests, **2021**.

[198] Dave Muoio, "FDA gives Cue Health first EUA for at-home, OTC COVID-19 molecular testing," can be found under https://www.mobihealthnews.com/news/fda-gives-cue-health-first-eua-home-otc-covid-19-molecular-testing, **2021**.

[199] G. Ruiz-Vega, M. Soler, L. M. Lechuga, *J. Phys. Photonics* **2021**, *3*, 011002.

[200] H. C. Ates, A. K. Yetisen, F. Güder, C. Dincer, *Nat. Electron.* **2021**, *4*, 13.

[201] P. Q. Nguyen, L. R. Soenksen, N. M. Donghia, N. M. Angenent-Mari, H. de Puig, A. Huang, R. Lee, S. Slomovic, T. Galbersanini, G. Lansberry, H. M. Sallum, E. M. Zhao, J. B. Niemi, J. J. Collins, *Nat. Biotechnol.* **2021**, *39*, 1366.

[202] D. Maier, E. Laubender, A. Basavanna, S. Schumann, F. Güder, G. A. Urban, C. Dincer, *ACS Sens.* **2019**, *4*, 2945.

Gözde Kabay obtained her master's and doctoral degrees in Biomedical Engineering at TOBB University of Economics and Technology in Turkey. During her doctoral studies, she also conducted research at the University of Wisconsin-Madison. After her postdoctoral stay at FIT & IMTEK at the University of Freiburg, she is currently working as a group leader at the Institute of Functional Interfaces, Karlsruhe Institute of Technology. Her main research interests include various fields ranging from biosensors, biomaterials, drug delivery, and plasma processing of materials for biomedical applications.

**ADVANCED
SCIENCE NEWS**

www.advancedsciencenews.com

**ADVANCED
MATERIALS**

www.advmat.de

Jonalyn DeCastro obtained her master's degree in Applied Life Sciences and is currently pursuing her doctoral degree in Bioengineering at Keck Graduate Institute - The Claremont Colleges in understanding the effects of blood on aging. She also works as a visiting researcher at the University of California - Berkeley at the Department of Bioengineering. Her main interests include various fields ranging from biosensors, developing organ-on-a-chip microphysical systems, and pursuing novel innovations for point-of-care, biomedical solutions that intersect biology and engineering technologies.

Alara Altay is a master student in the "Disposable Microsystems" group at FIT and IMTEK, University of Freiburg. She obtained her bachelor's degree in Mechatronics Engineering with a minor in Energy at the Sabanci University in Turkey. In the summer of 2018, she also worked as a visiting student at the Department of Microengineering, Swiss Federal Institute of Technology Lausanne (EPFL). Her current research focuses on wearable and point-of-care sensors for diagnostics and health monitoring.

Kiana Aran is an associate professor of Bioengineering at Keck Graduate Institute and the co-founder and chief scientific officer at Cardea Bio. Her research efforts focus on designing novel biosensing platforms for early disease diagnosis as well as utilizing biology as tech elements for a variety of biosensing applications. She has been recognized within the scientific community by the Clinical OMICs 10 under 40 Award, Athena Pinnacle Award in Life Sciences, and Nature Research Awards for Inspiring Women in Science. Dr. Aran is also the recipient of numerous government grants to develop the next generation of electronic biosensors.

Can Dincer is a junior research group leader at FIT and IMTEK at the University of Freiburg. He received his doctoral degree with summa cum laude in microsystems engineering from the University of Freiburg. Between June 2017 and June 2019, he also worked as a visiting researcher at the Department of Bioengineering at the Imperial College London. The main interest of his research group "Disposable Microsystems" is the development of bioanalytical materials/sensors/microsystems and their combination with data science and artificial intelligence for various applications including diagnostics, especially for point-of-care diagnostics and wearables, food and environmental monitoring.